Control and Interconnection Issues of AC and DC Microgrids

Rosa A. Mastromauro

Politecnico di Bari

Italy

rosaanna.mastromauro@poliba.it

Outline

A **MICROGRID** is an electrical system that includes multiple loads and distributed energy resources that can be operated in parallel with main grid or as an electrical island.

In the Distributed Generation scenario, the **MICROGRID** concept has been introduced as a solution to provide high power quality and to improve the reliability of the traditional electrical power system.

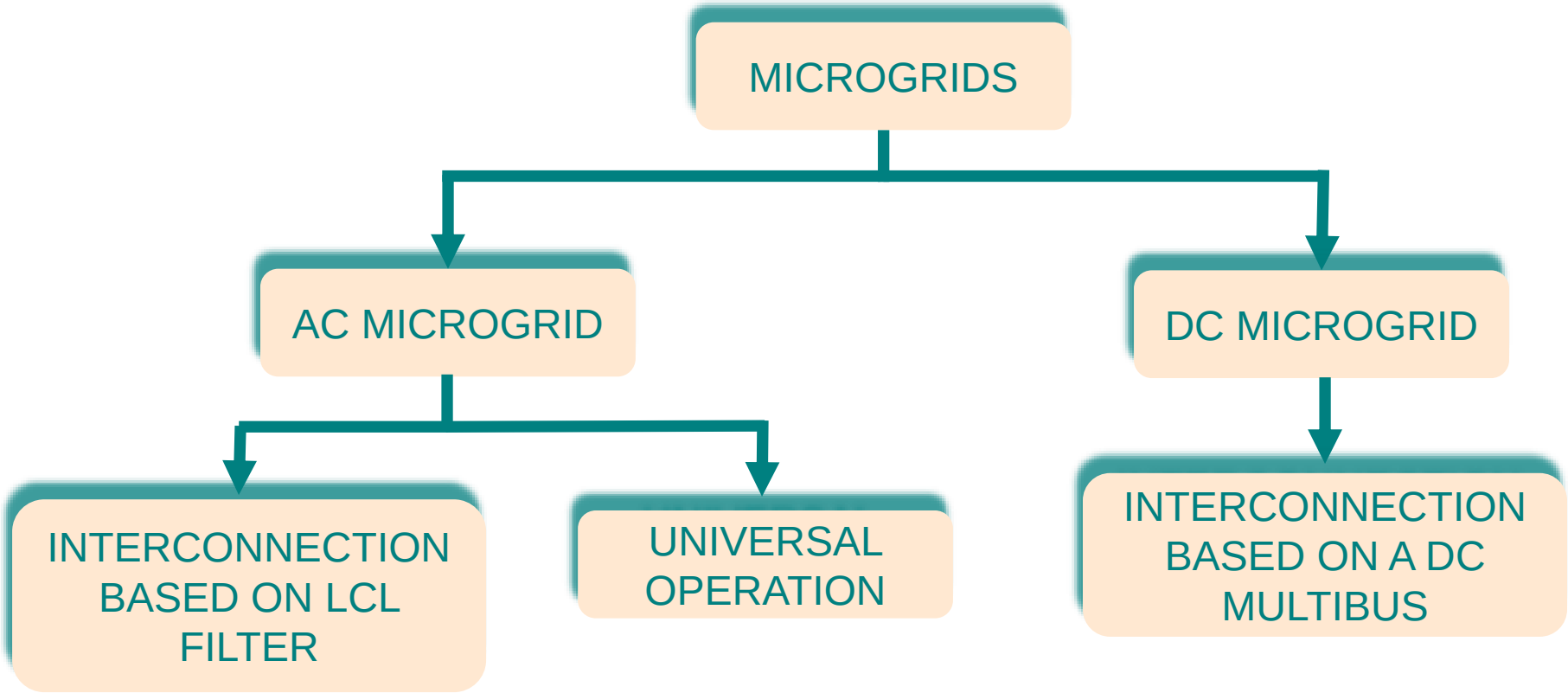

rosaanna.mastromauro@poliba.it

Interconnection based on LCL Filter: Damping Methods for the Control of Grid-Connected Converters

rosaanna.mastromauro@poliba.it

Damping Methods for the Control of Grid-Connected Converters

In DPGS applications the grid filter has a fundamental role because since it represents the front-end between the inverter and the grid.

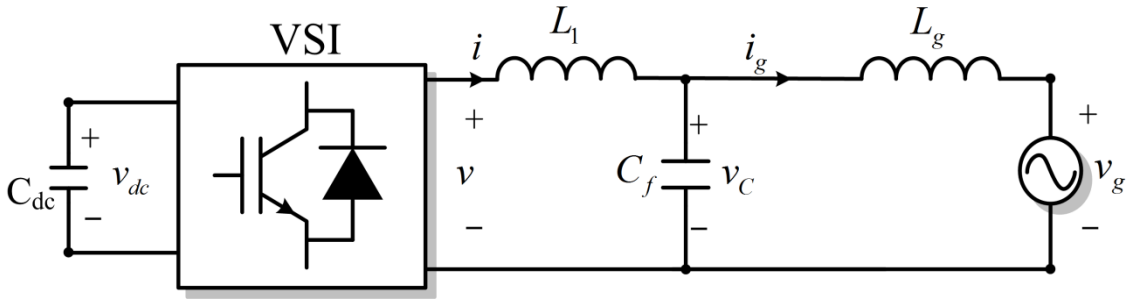

The LCL filter is used for reducing the PWM harmonics due to its good filtering characteristic.
The drawback of the LCL-filter is its peak gain at the resonance frequency.

Passive damping

Passive damping is realized by addition of circuital components in the system and this method causes a decrease of the overall system efficiency.

Active damping

Active damping methods consist in modifying the controller, they are more selective in their action and do not produce losses but they are also more sensitive to parameters uncertainties.

Damping Methods for the Control of Grid-Connected Converters

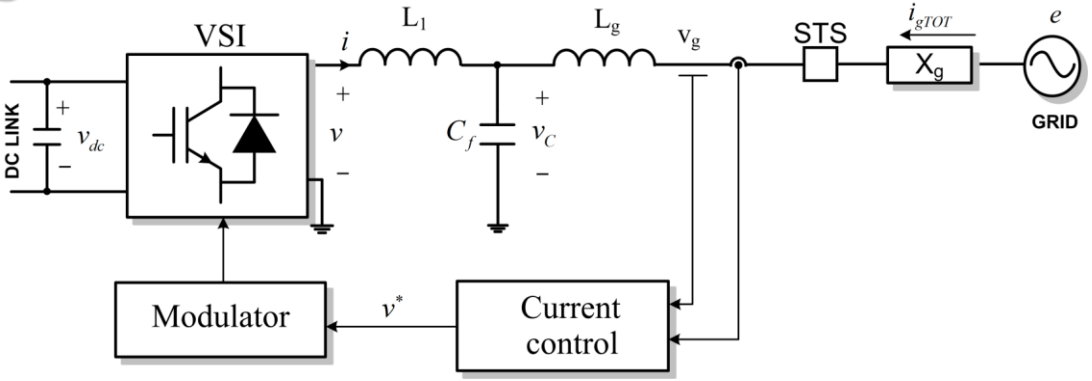

The current control can be implemented in two different ways

Grid current control

$$G_{IL} = \frac{I_L}{V_C} = \frac{1}{L_1 L_g C_f s} \frac{1}{s^2 + \omega_{Res}^2}$$

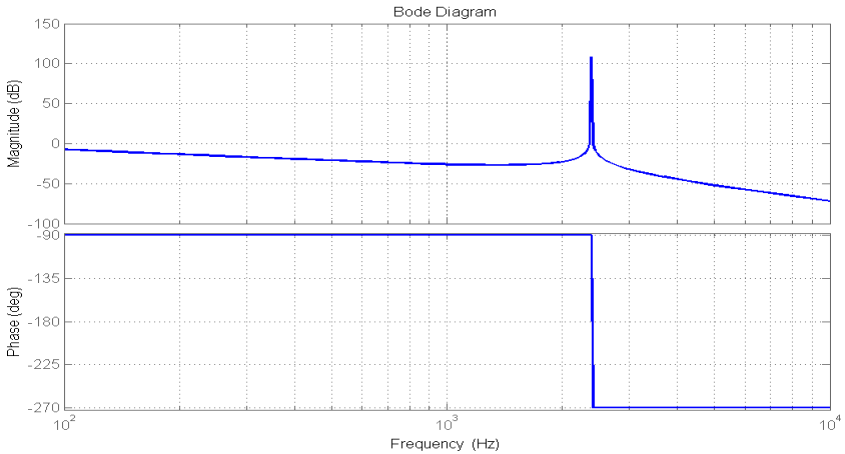

Converter current control

$$G_{IC} = \frac{I_C(s)}{V_C(s)} = \frac{1}{L_1 s} \frac{s^2 + \omega_0^2}{s^2 + \omega_{Res}^2}$$

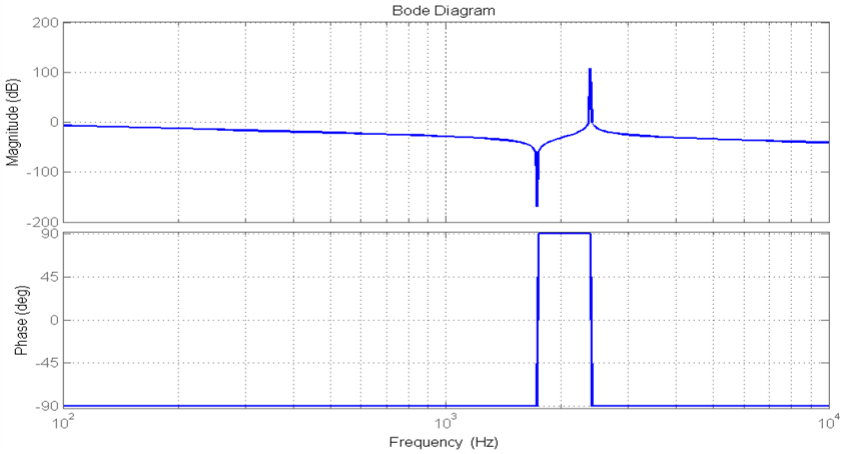

Active Damping of the LCL Filter

Active damping consists in modifying the controller parameters without adding extra losses. Active damping methods are more selective in their action, they do not produce losses but they are also more sensitive to parameter uncertainties.

- Multi-loop
  - Lead network
  - Virtual Resistor
- Filter
  - Bi quadratic filter
  - Notch Filter

The stability is guaranteed via the control of more system state variables that are measured or estimated.

This class of active damping methods does not need more sensors.

rosaanna.mastromauro@poliba.it

Active Damping of the LCL Filter: Notch and Bi-quadratic Filter

The ***Notch filter*** based active damping introduces a negative peak in the system that compensates the resonant peak due to the LCL filter.

A ***Bi-quadratic filter*** has two poles and two zeros in order to reduce the resonance peak of the LCL-filter.

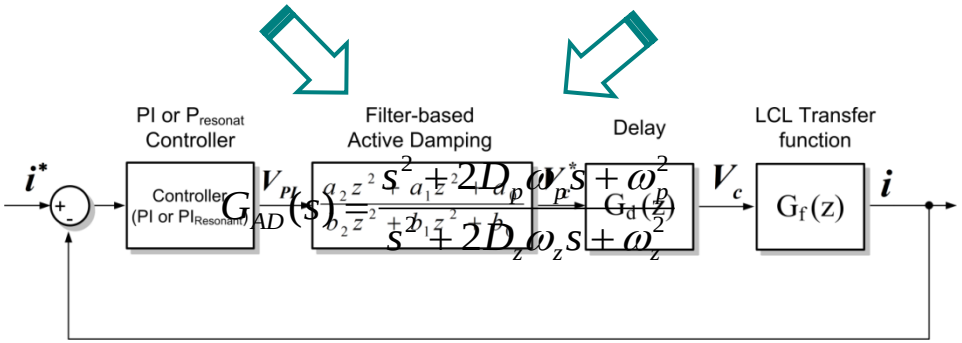

Bode diagram of Notch filter

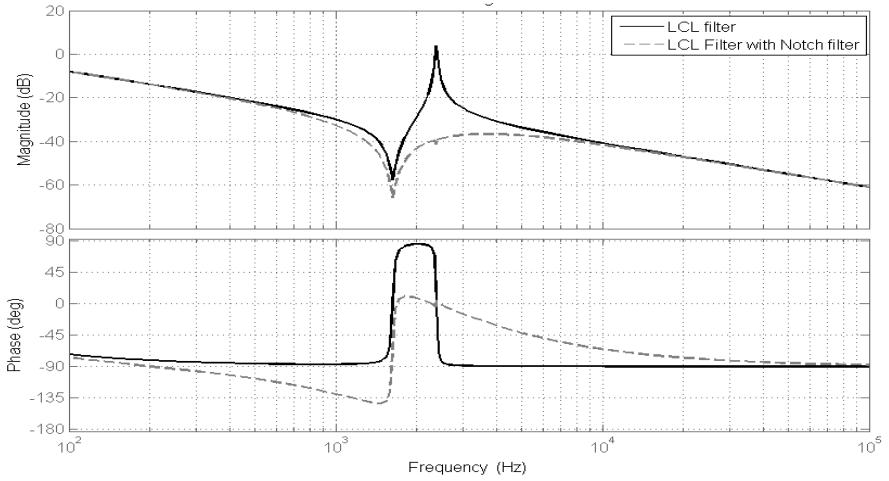

Bode diagram of Bi-quadratic filter

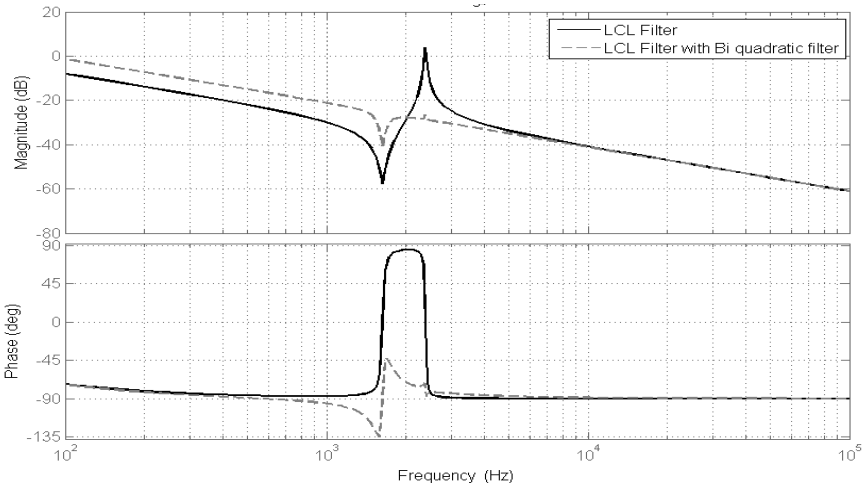

rosaanna.mastromauro@poliba.it

Active Damping of the LCL Filter: Virtual Resistor

Active damping with ***Virtual Resistor*** consists of adding a virtual resistance in series to the capacitor. This method introduces a virtual resistance but it does not produce Joule losses

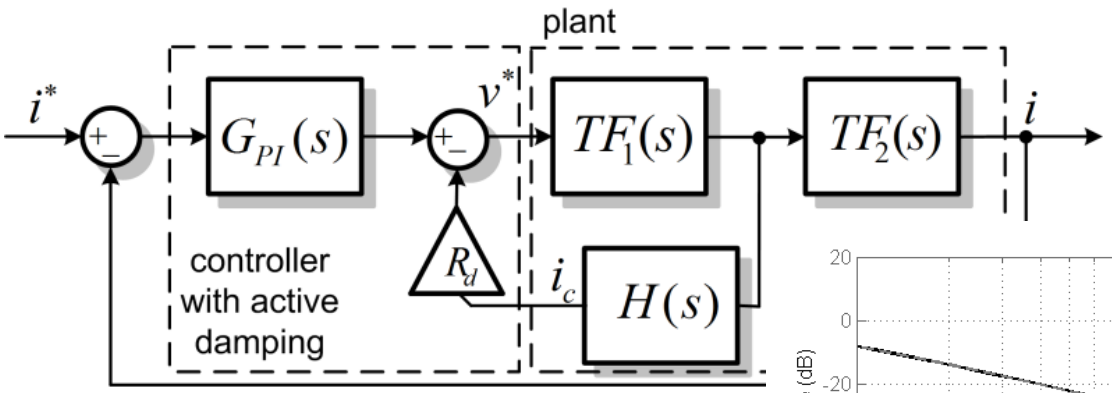

$$R_v = R_d \frac{(L_1 + L_g)}{L_g}$$

$$TF_1(s) = \frac{L_g C s^2 + R_g C s}{L_g L_1 C s^3 + (R_1 L_g C + L_1 C R_g) s^2 + (C R_g R_1 + L_g + L_1) s +}$$

$$TF_2(s) = \frac{L_g C s^2 + R_g C s + 1}{L_g C s^2 + R_g C s}$$

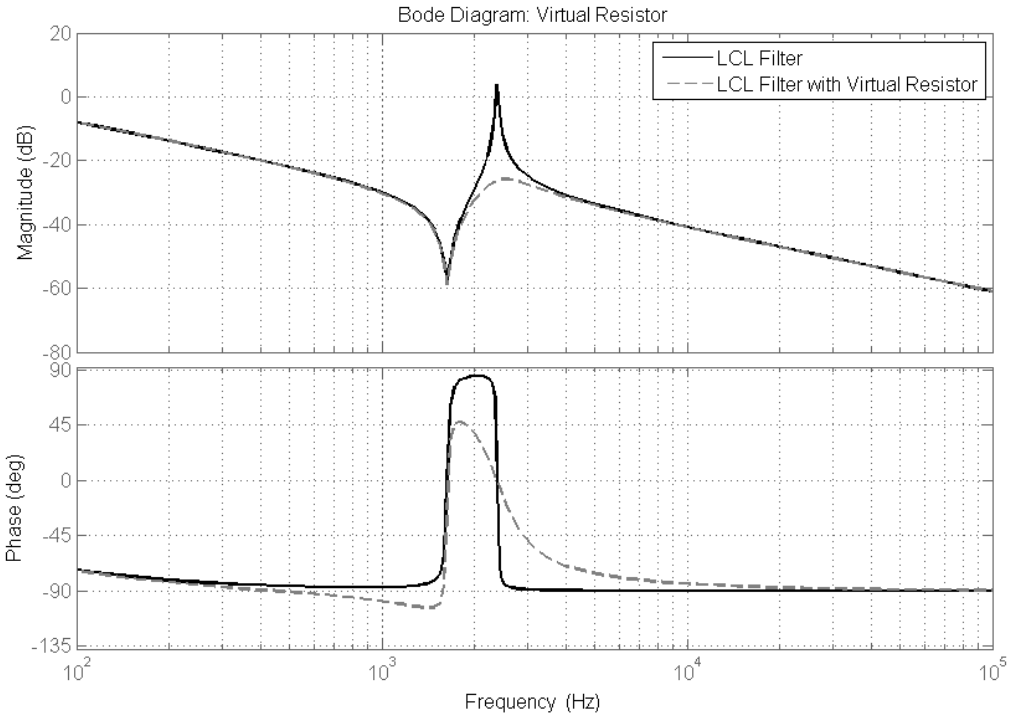

Active Damping of the LCL Filter: Lead Network

The ***Lead Network*** active damping method consists of the LCL filter voltage capacitor (V_c) control.

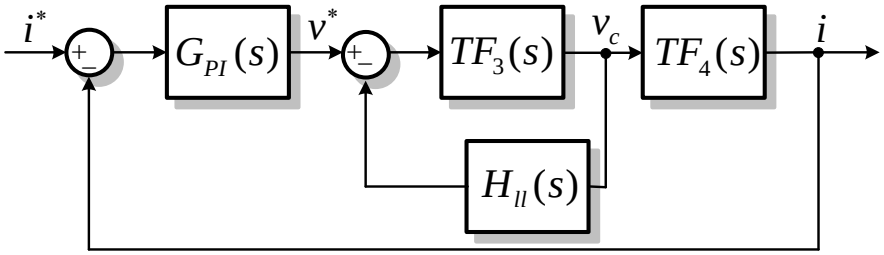

$$TF_4(s) = \frac{I(s)}{V_c(s)} = \frac{1}{L_g s}\frac{s^2 + Z_{LC}^2}{Z_{LC}^2}$$

$$TF_3(s) = \frac{V_c(s)}{V(s)} = \frac{L_g}{L_1}\frac{Z_{LC}^2}{s^2 + \omega_{RES}^2}$$

$$H_{ll}(s) = k_d C \omega_{max}\left(\frac{s + k_f \omega_{max}}{k_f s + \omega_{max}}\right)$$

$$k_f = \sqrt{\frac{1 - \sin\varphi_{max}}{1 + \sin\varphi_{max}}}$$

It introduces a phase gain around the resonance frequency

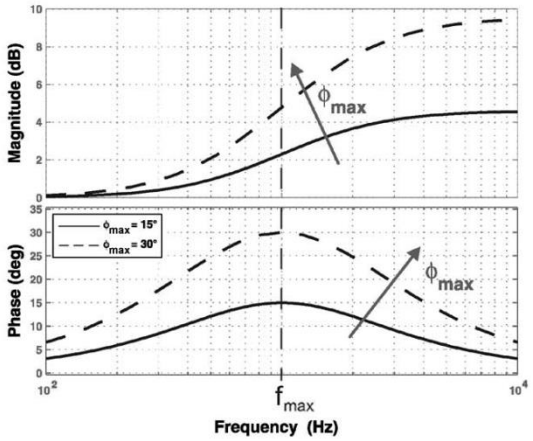

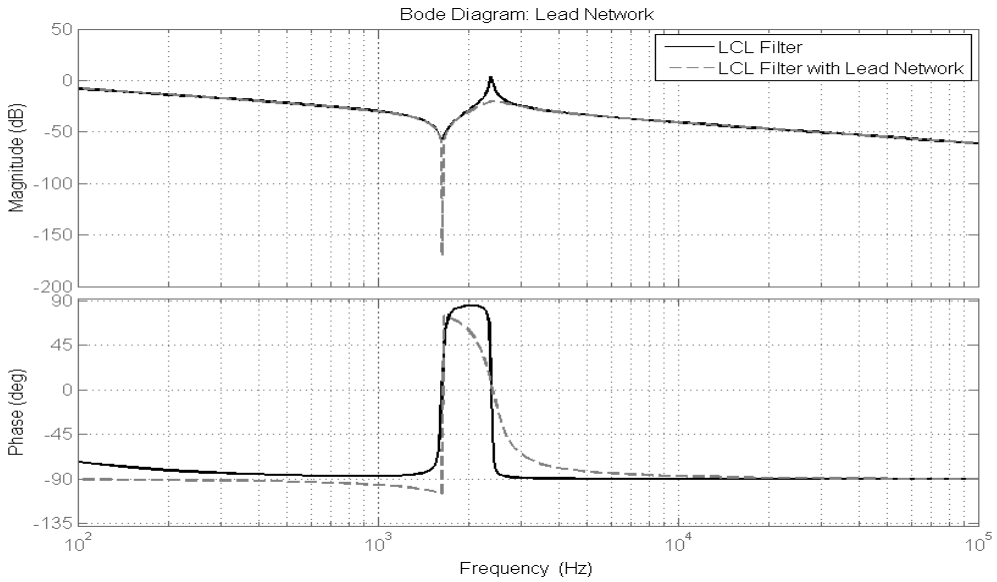

rosaanna.mastromauro@poliba.it

Traditional Control System of the Grid-Connected Converter

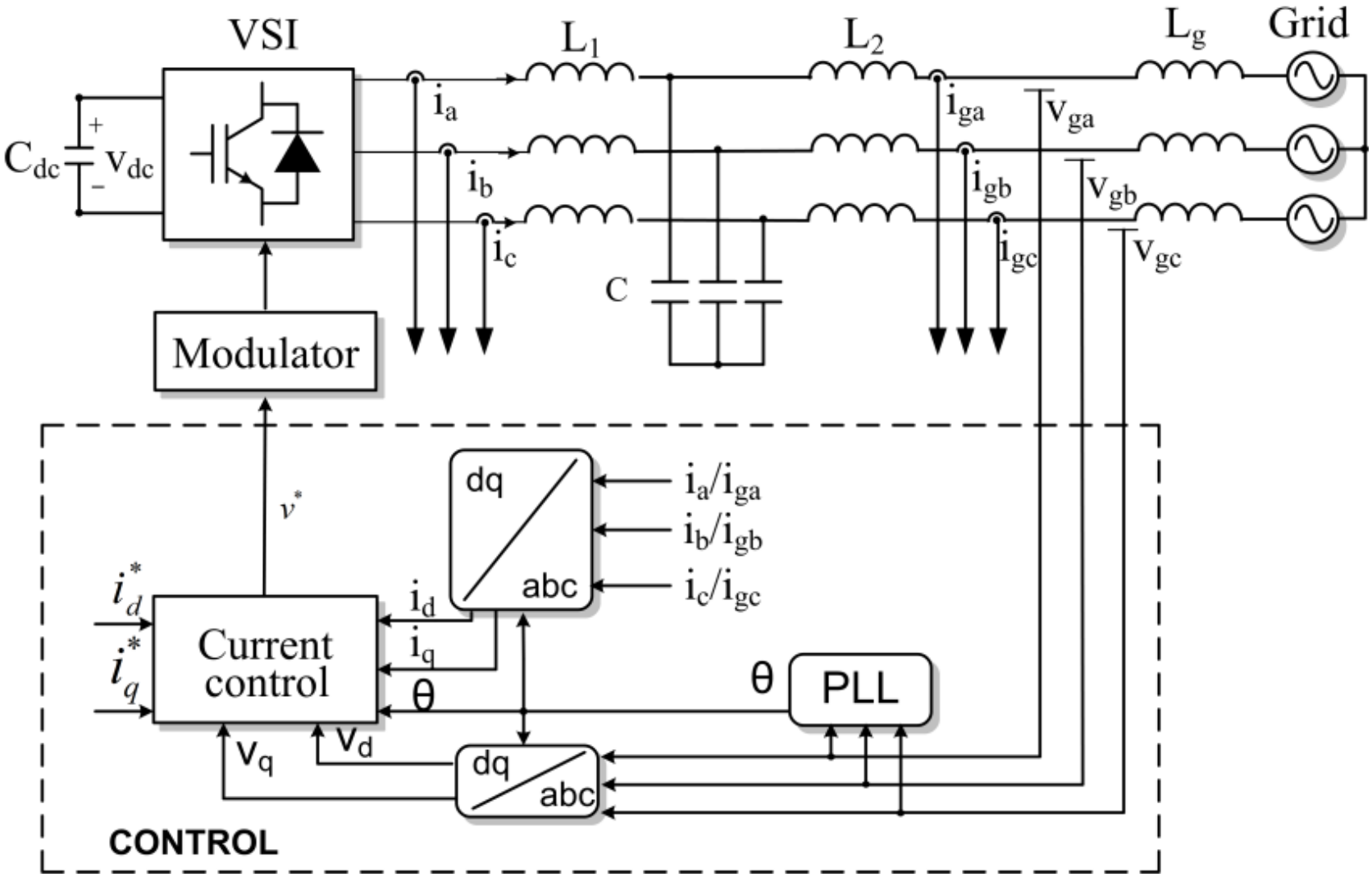

Experimental Setup

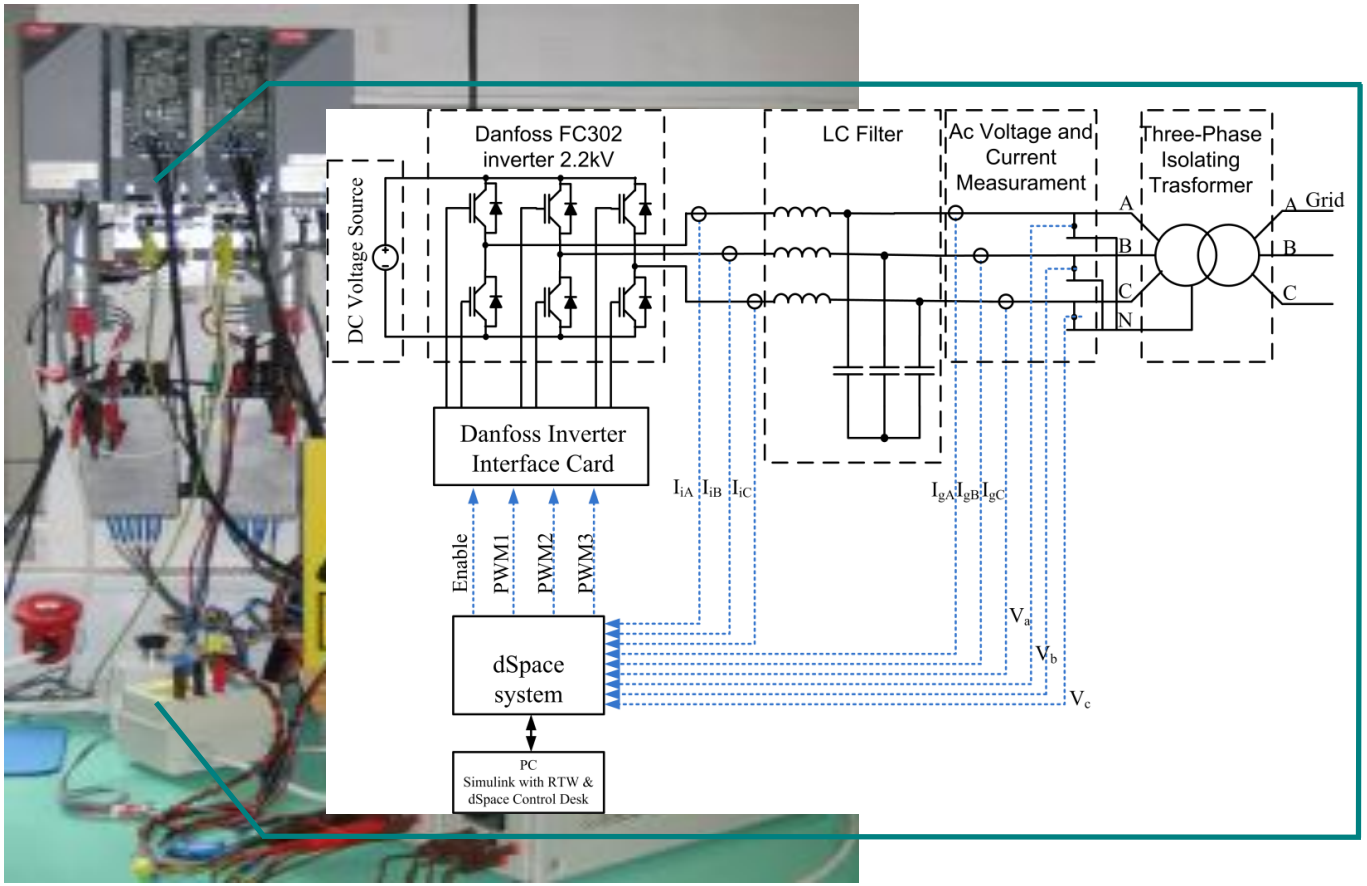

rosaanna.mastromauro@poliba.it

Damping Methods for the Control of Grid-Connected Converters: Results

Results when the **Notch filter** is enabled

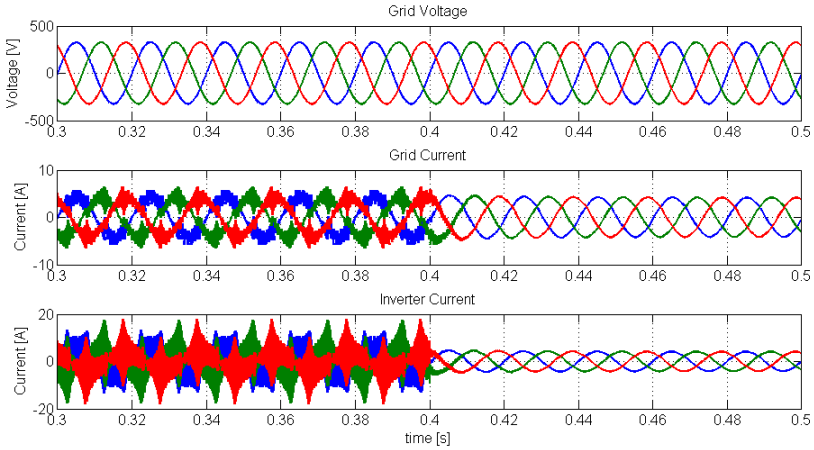

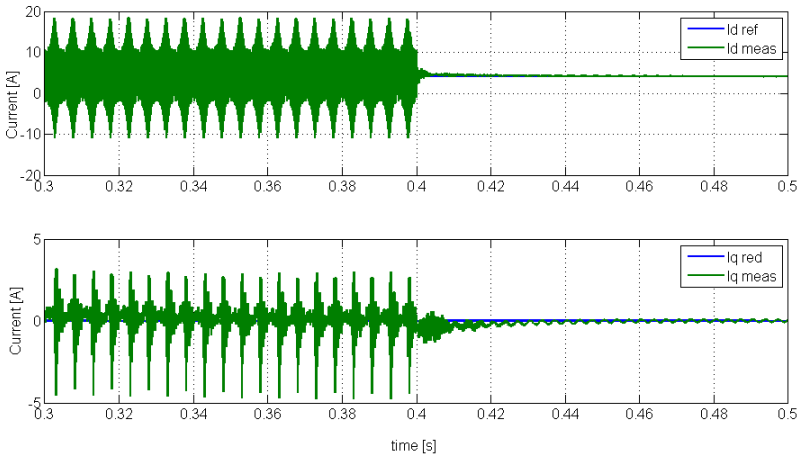

Results when the **Bi-quadratic filter** is enabled

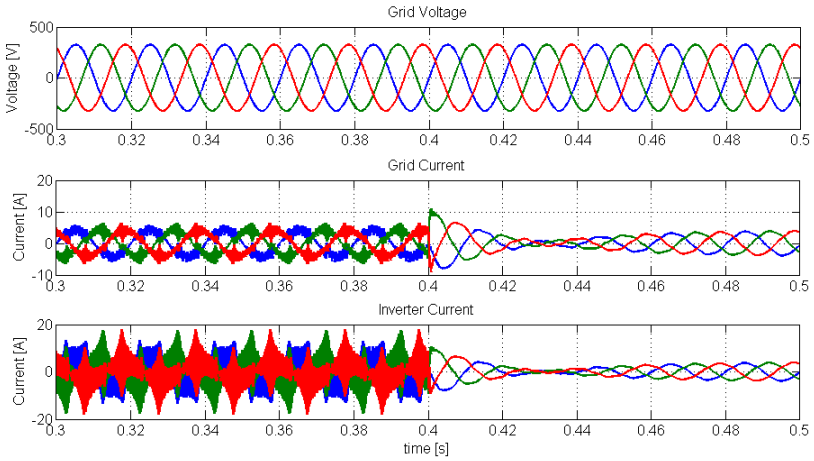

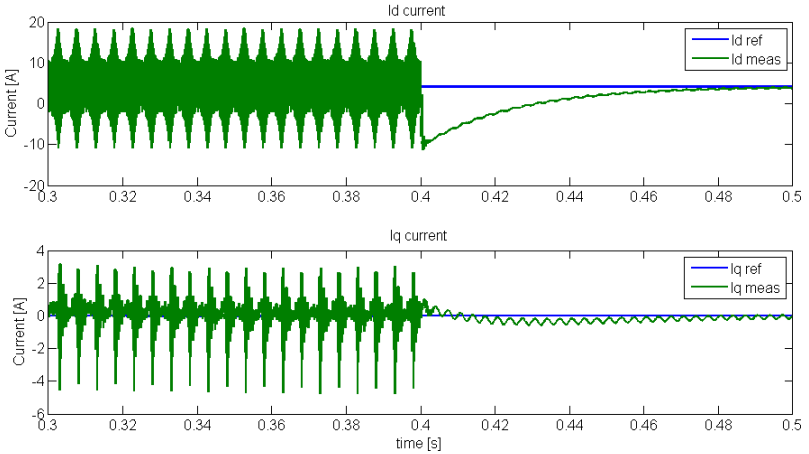

rosaanna.mastromauro@poliba.it

Damping Methods for the Control of Grid-Connected Converters: Simulation Results

Simulation results when the **Virtual resistor** is enabled

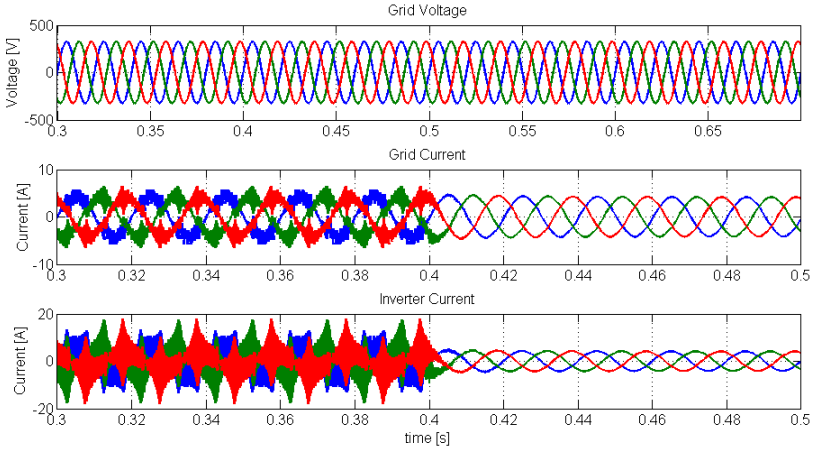

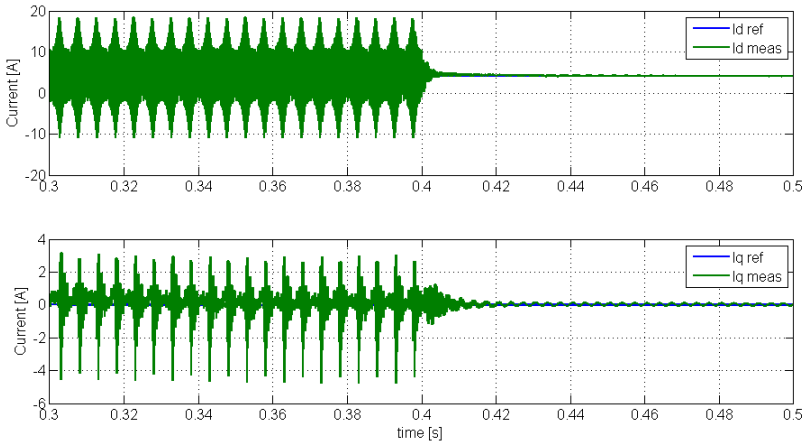

Simulation results when the **Lead network** is enabled

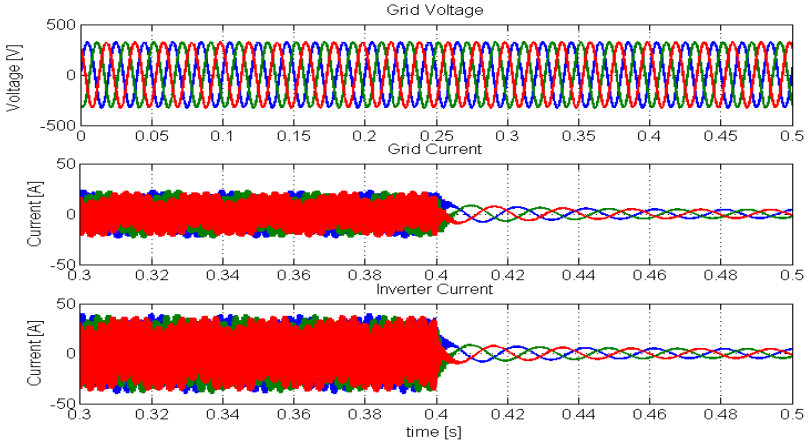

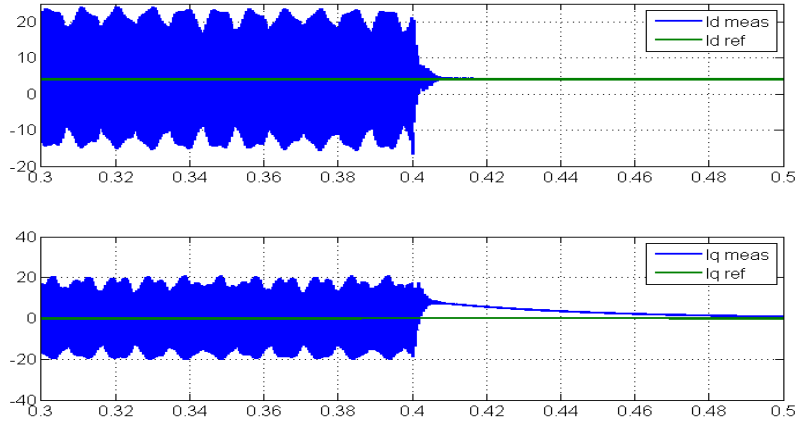

rosaanna.mastromauro@poliba.it

Robust analysis of Active Damping Methods

Robustness is the persistence of a system characteristic behavior under perturbations or unusual or conditions of uncertainty.

A control system is ROBUST if it is not very sensitive to differences between the real system and the model system that was used during the synthesis and design of the controller.

In order to analyze the robust stability properties it is necessary to define a sensitivity function

$$S(j\omega) = \frac{1}{1 + C(j\omega)G(j\omega)}$$

C(s) is the controller transfer function

$$G(j\omega) = G_n(j\omega) + \delta G(j\omega)$$

A high value of S(jω) indicates that the Nyquist diagram is near to the unstable condition.

rosaanna.mastromauro@poliba.it

Robust analysis of Active Damping Methods

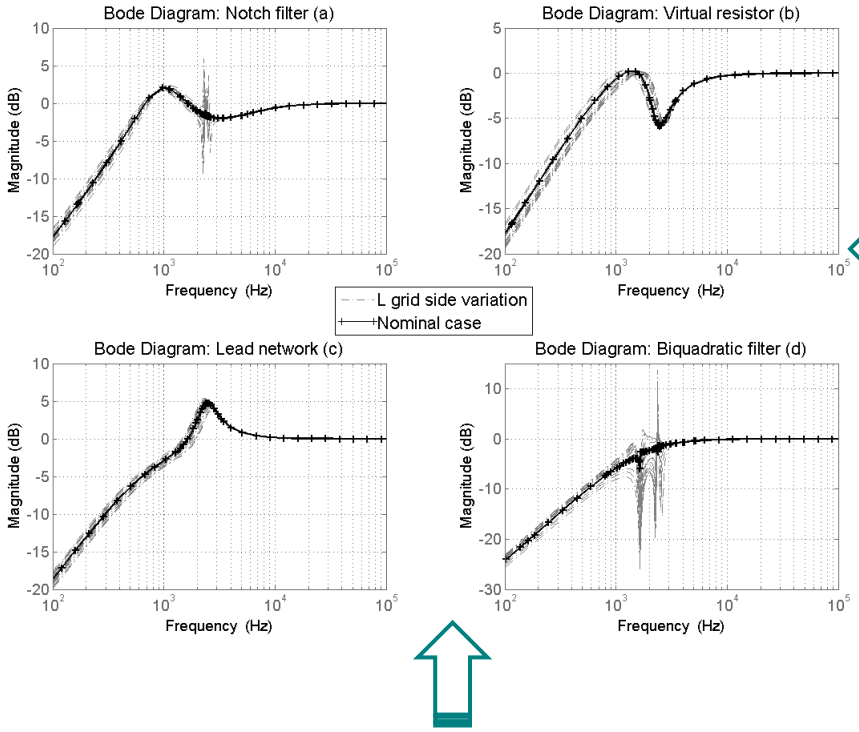

The Virtual Resistor method and Lead Network method are more robust than the others active damping methods because the resonance peak by the sensitivity function (S_M) is smaller than Notch filter and Bi-quadratic filter.

The Notch filter method and Bi-quadratic method are not robust in the case of large variation of the parameters due to these methods are designed in the case of nominal values.

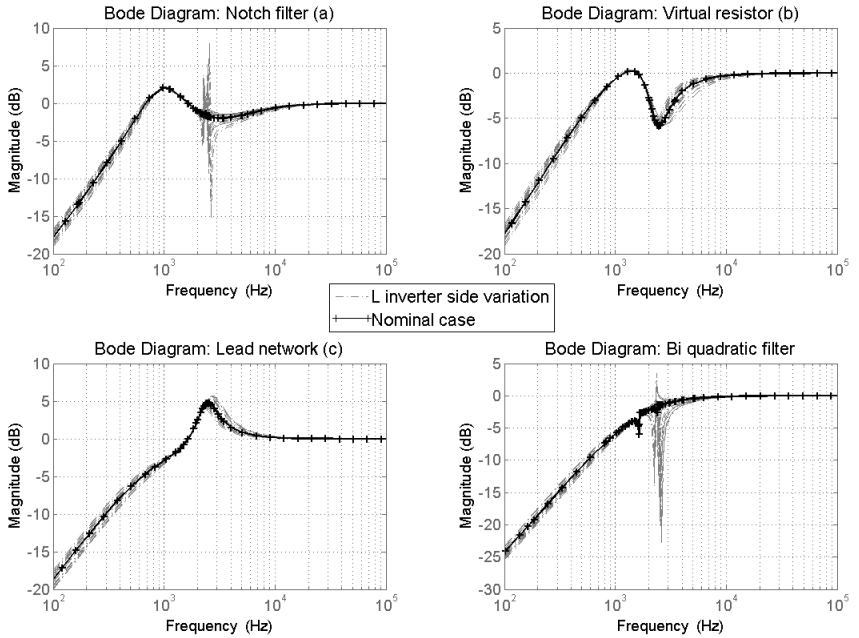

Simulation Results of the LCL Filter Control for Robustness Analysis

Nominal Parameters

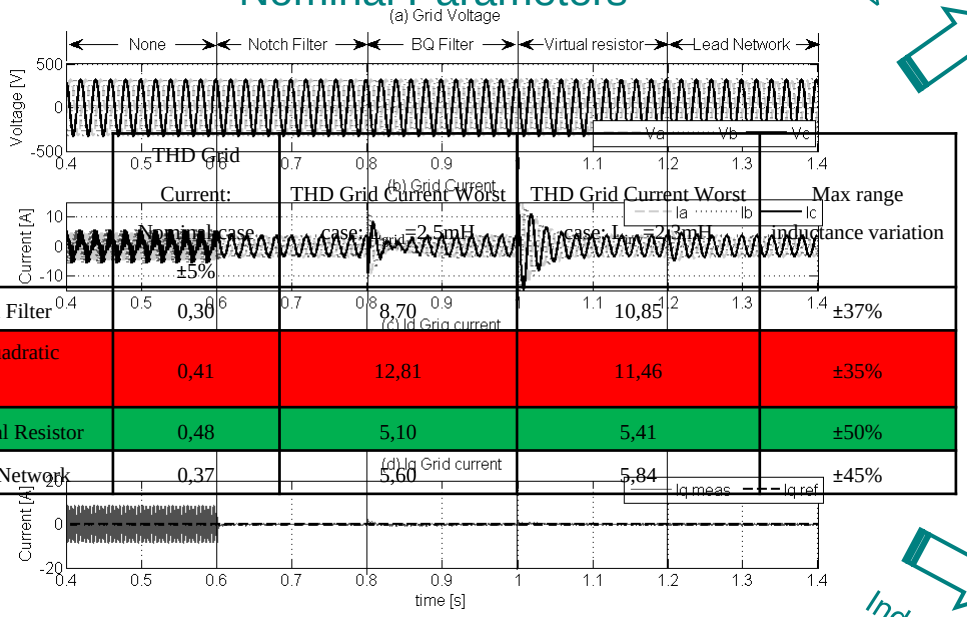

	Current: THD Grid	THD Grid Current Worst case: L_{grid} =2.5mH	THD Grid Current Worst case: L_{grid} =2.3mH	Max range inductance variation
Nominal case	±5%			
Notch Filter	0,30	8,70	10,85	±37%
Bi-Quadratic Filter	0,41	12,81	11,46	±35%
Virtual Resistor	0,48	5,10	5,41	±50%
Lead Network	0,37	5,60	5,84	±45%

Inductance grid side variation

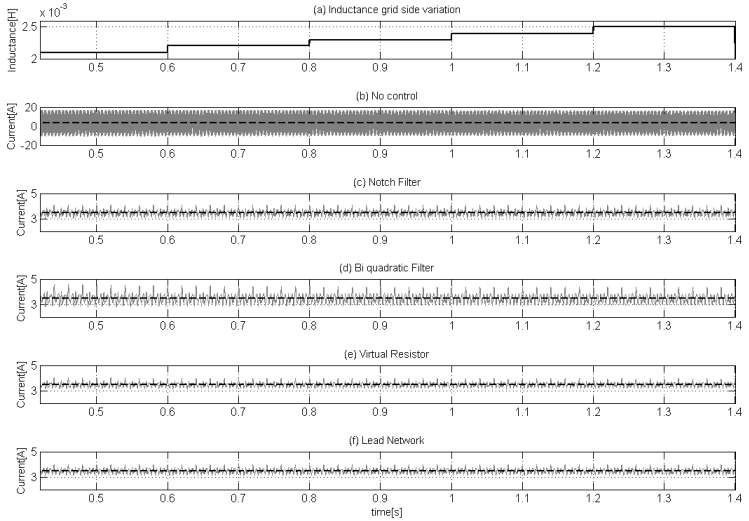

Inductance inverter side variation

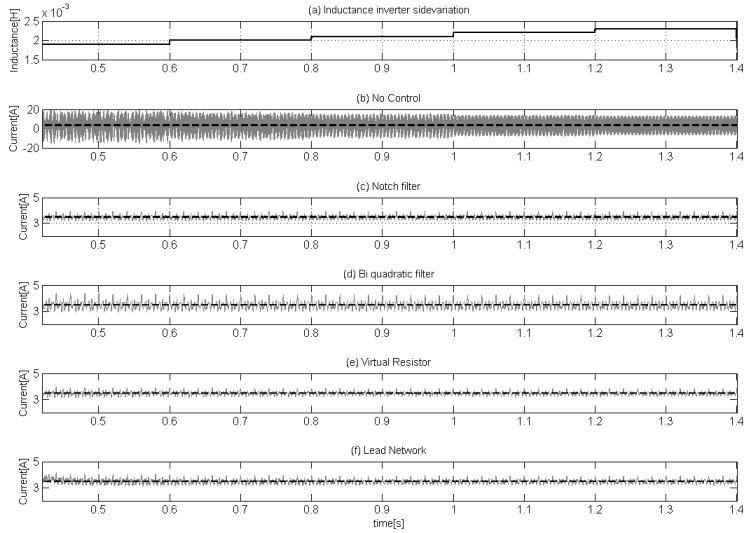

Comparison of the active Damping Methods Based on the Dynamic Performance

The dynamic performances of all the presented active damping methods have been investigated.

	Margin Gain [dB]	Margin Phase [°]	Settling Time [ms]	Overshoot [%]	PI proportional gain K_p
Detuned controller without active damping	1.01				
Notch filter	2.71				
Virtual Resistor (2 ohm)	1.83				
Bi-quadratic filter	1.24	7			
Lead Network	1.31				

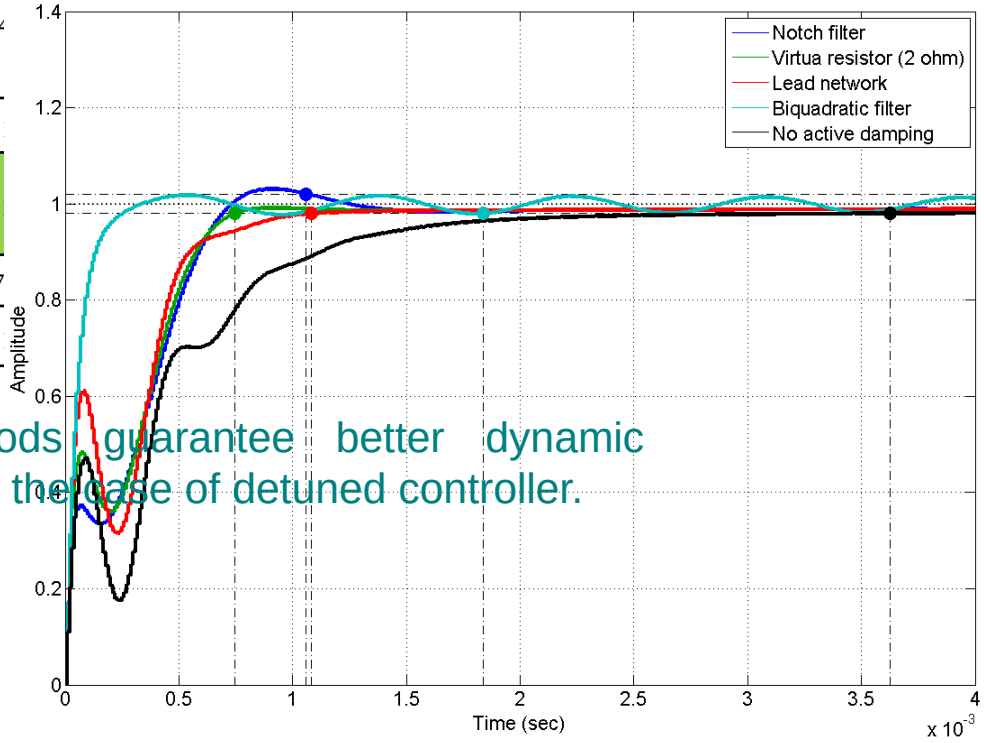

Active damping methods guarantee better dynamic performances respect to the case of detuned controller.

The ***Virtual Resistor*** results the best solution both in terms of dynamic response and overshoot, followed by the *Lead Network* method which is slower than the first one.

Simulation Results about the Dynamic Performance of the Active Damping Methods

Active power reference step from 500 W to 2 kW

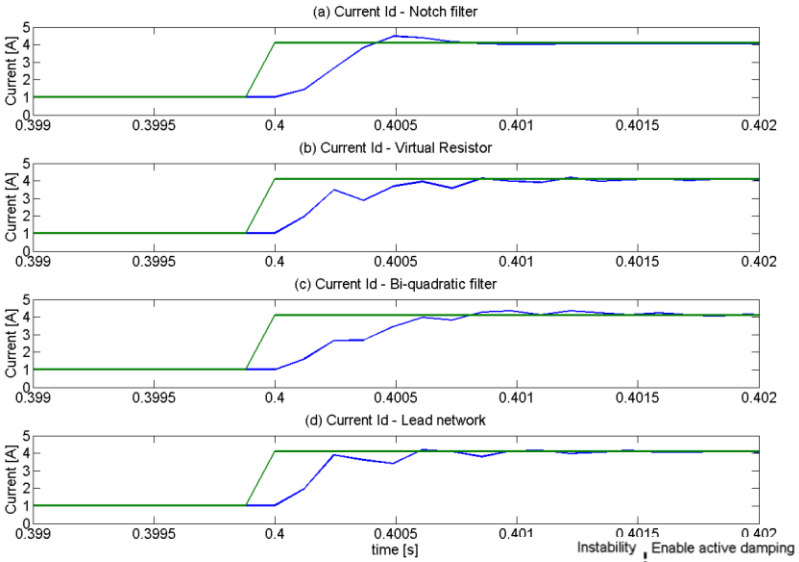

Grid current in case of active damping insertion

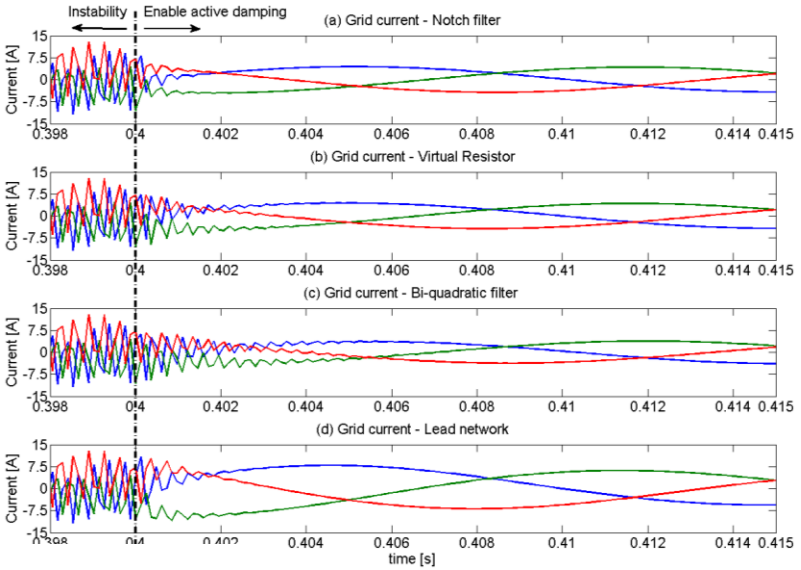

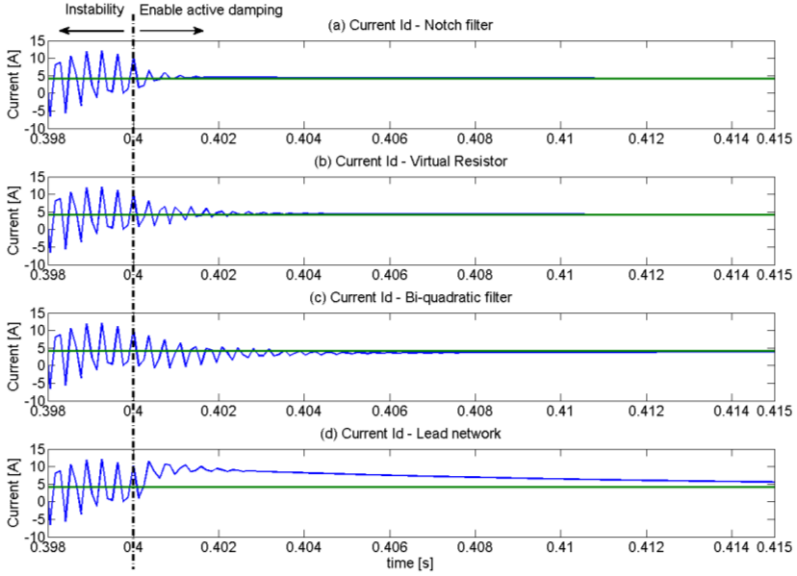

I_d current in case of active damping insertion (starting from instability condition)

Experimental Results about the Dynamic Performance of the Active Damping Methods

Notch filter

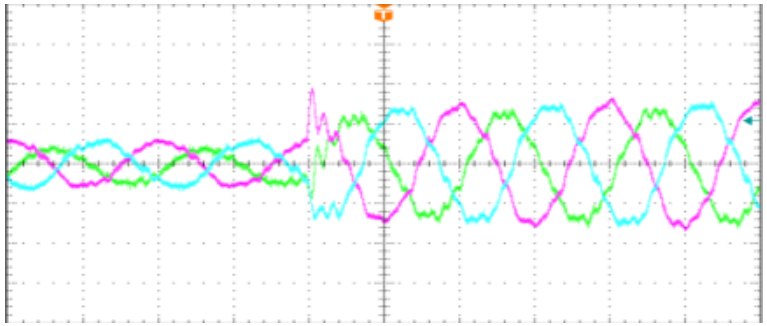

Virtual Resistor (R_v=2 ohm)

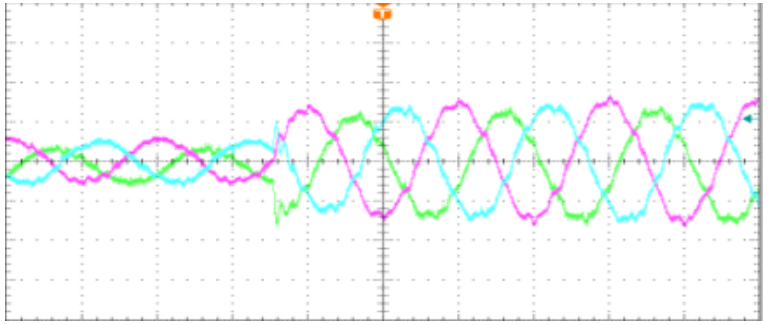

Bi-quadratic filter

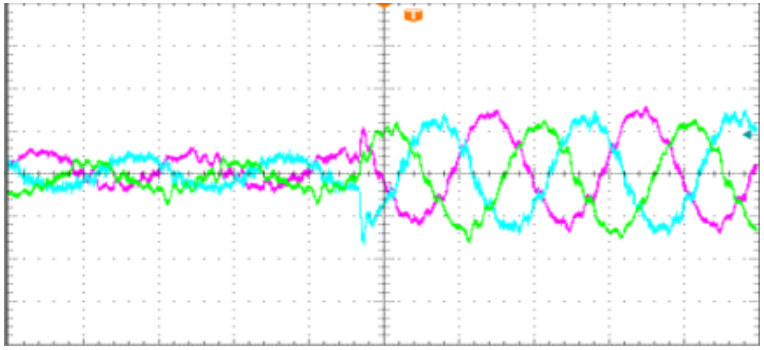

Lead Network

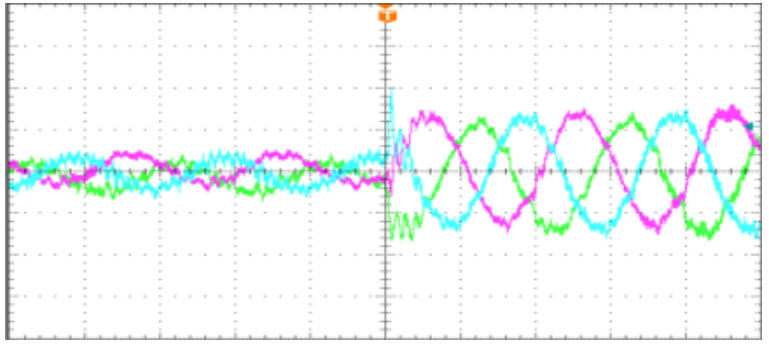

rosaanna.mastromauro@poliba.it

Universal Operation of a Distributed Power Generation System Based on the Power Converter Control

rosaanna.mastromauro@poliba.it

Universal Operation of a Distributed Power Generation System Based on the Power Converter Control

In the recent years the Electrical Power System is subjected to a restructuring process worldwide. Indeed, with deregulation, advancement in technologies and concern about the environmental impacts, increased interconnection of distributed power generation units to the main grid is fostered.

Distributed Power Generation Systems (DPGS)

Grid-connected mode

Islanding modes

No interruption in the load power supply

rosaanna.mastromauro@poliba.it

Grid-feeding and grid-forming converters

- Traditionally the DPGS are current controlled in grid-connected mode and they deliver a pre-specified amount of active power into the distribution network.

- Differently in stand-alone operation mode, or forming a microgrid, the DPGS are voltage controlled and are responsible for both voltage and power control, in this case the DPGS converters are grid-forming.

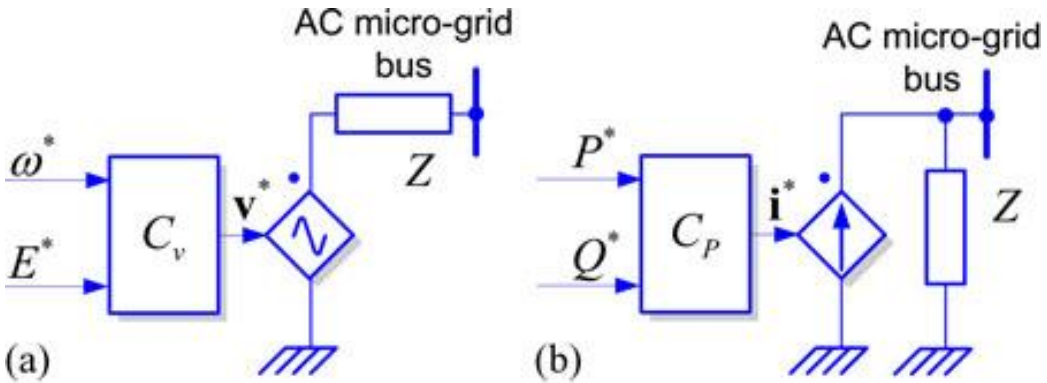

GRID-FORMING

It usually operates in islanded mode

GRID-FEEDING

It cannot operate in island mode

Microgrid configuration: a real case study

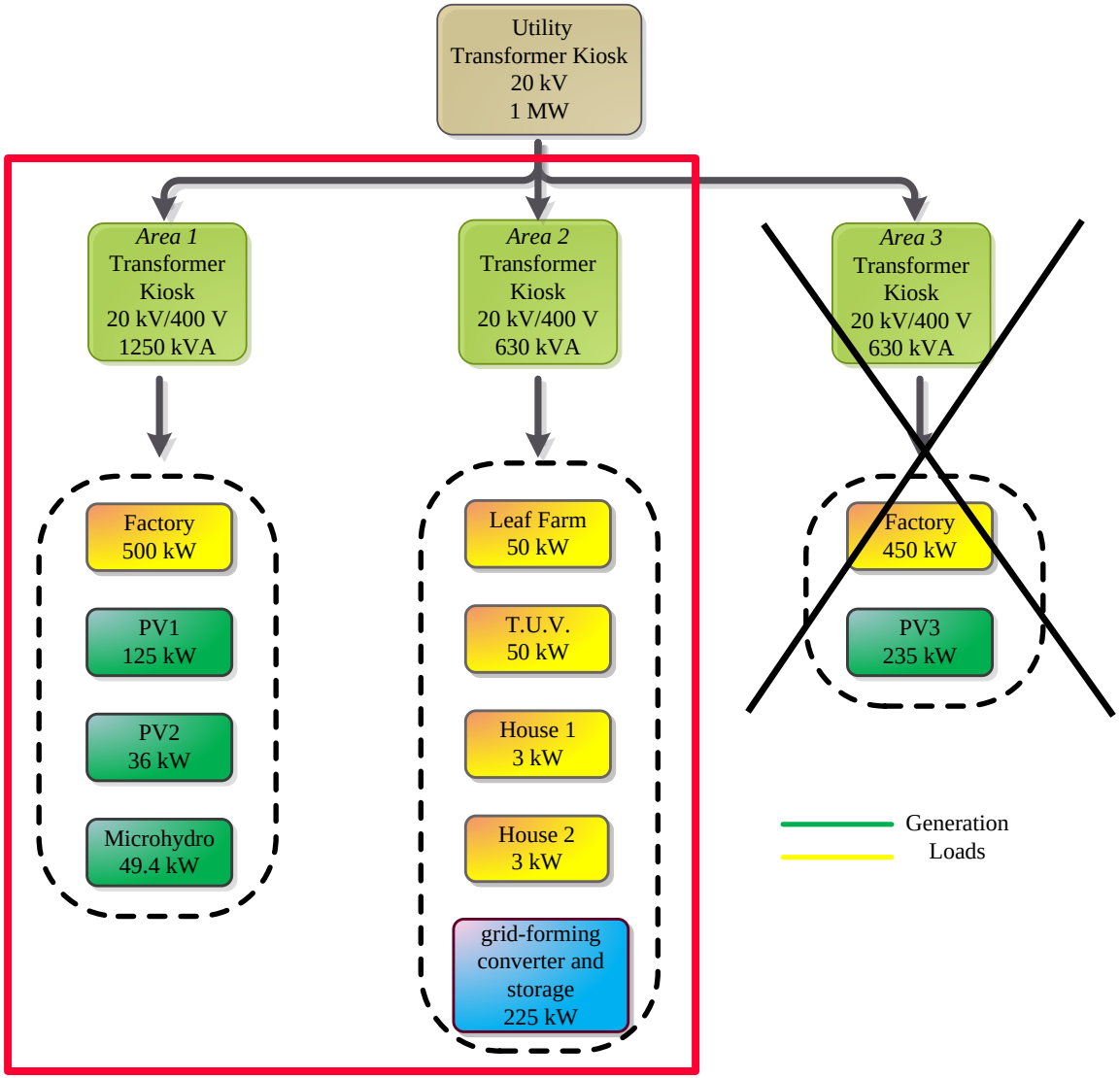

Grid-forming converter connected to the storage

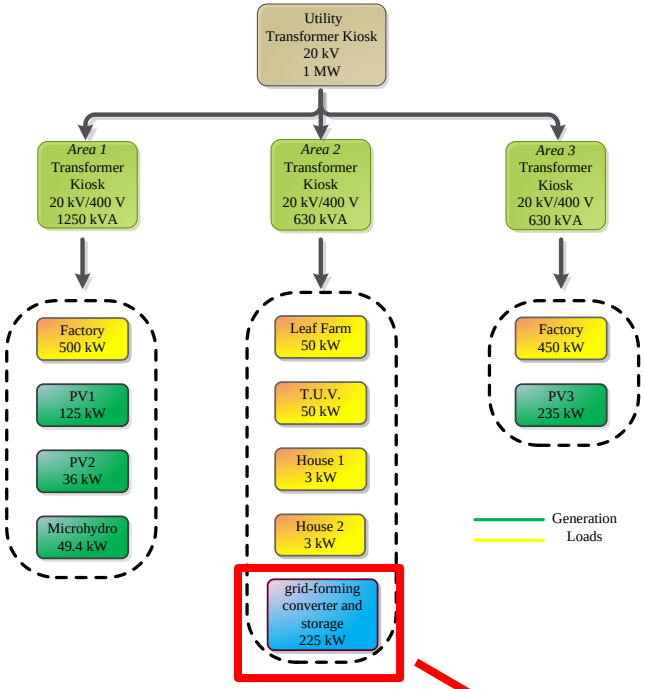

The AC voltage generated by the grid-forming converter is used as a reference for the rest of the grid-feeding converters connected to the microgrid.

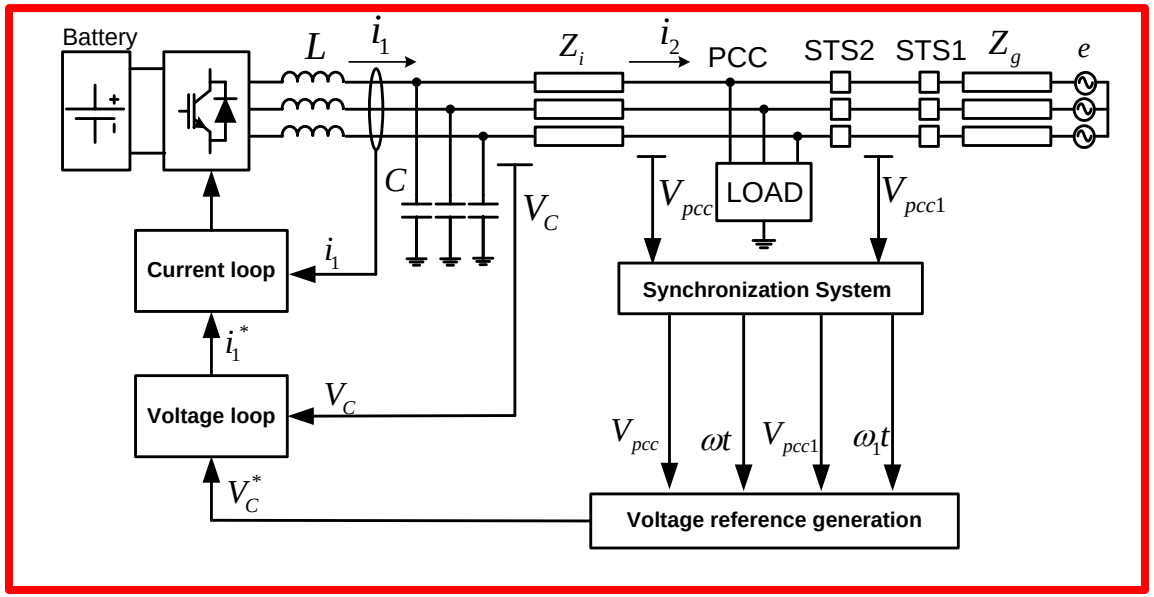

Rosa A. Mastromauro
rosaannamastromauro@poliba.it

Control of the grid-forming converter

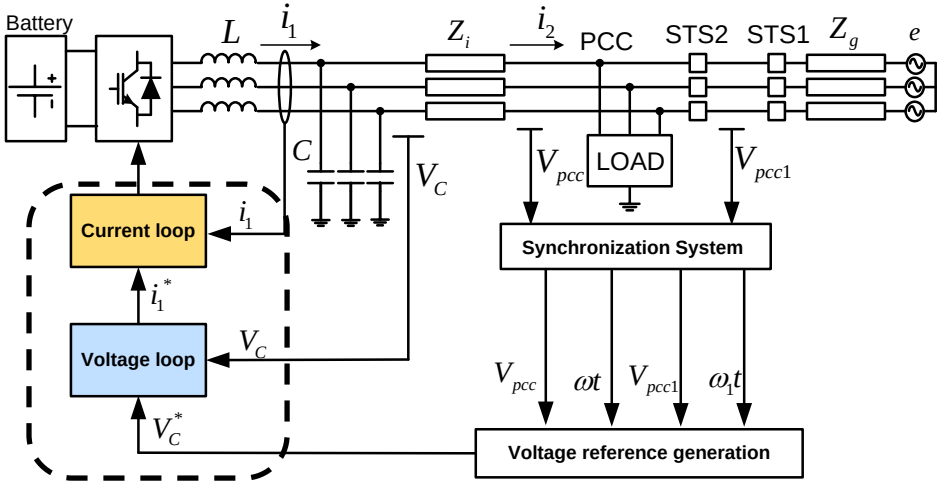

- In grid-connected operation the voltage reference may be synchronized with the main grid and two different PLLs are necessary in order to manage the grid-former converter may be communicated to the other inverters of both the undesired islanding conditions the microgrid in order to fulfil due to grid faults and the procedure of coordination of the plants.
- In stand-alone operation or intentional island the voltage angle of reconnection to the main grid. One PLL the grid-former converter may be is used for monitoring the grid and the other is used for the converter voltage to guarantee acceptable power quality supplying the loads and stability of the measured at the PCC.
overall system

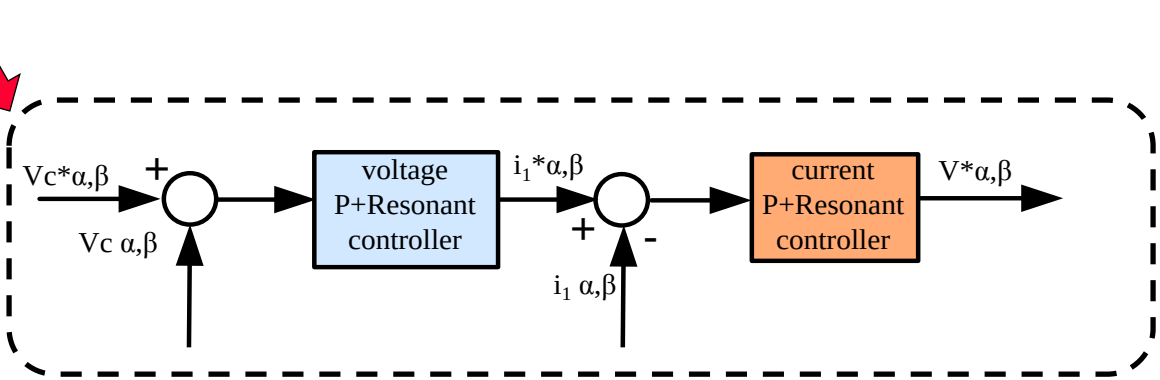

$$\begin{cases} p = v_\alpha i_{1\alpha} + v_\beta i_{1\beta} \\ q = v_\beta i_{1\alpha} - v_\alpha i_{1\beta} \end{cases}$$

Synchronization system

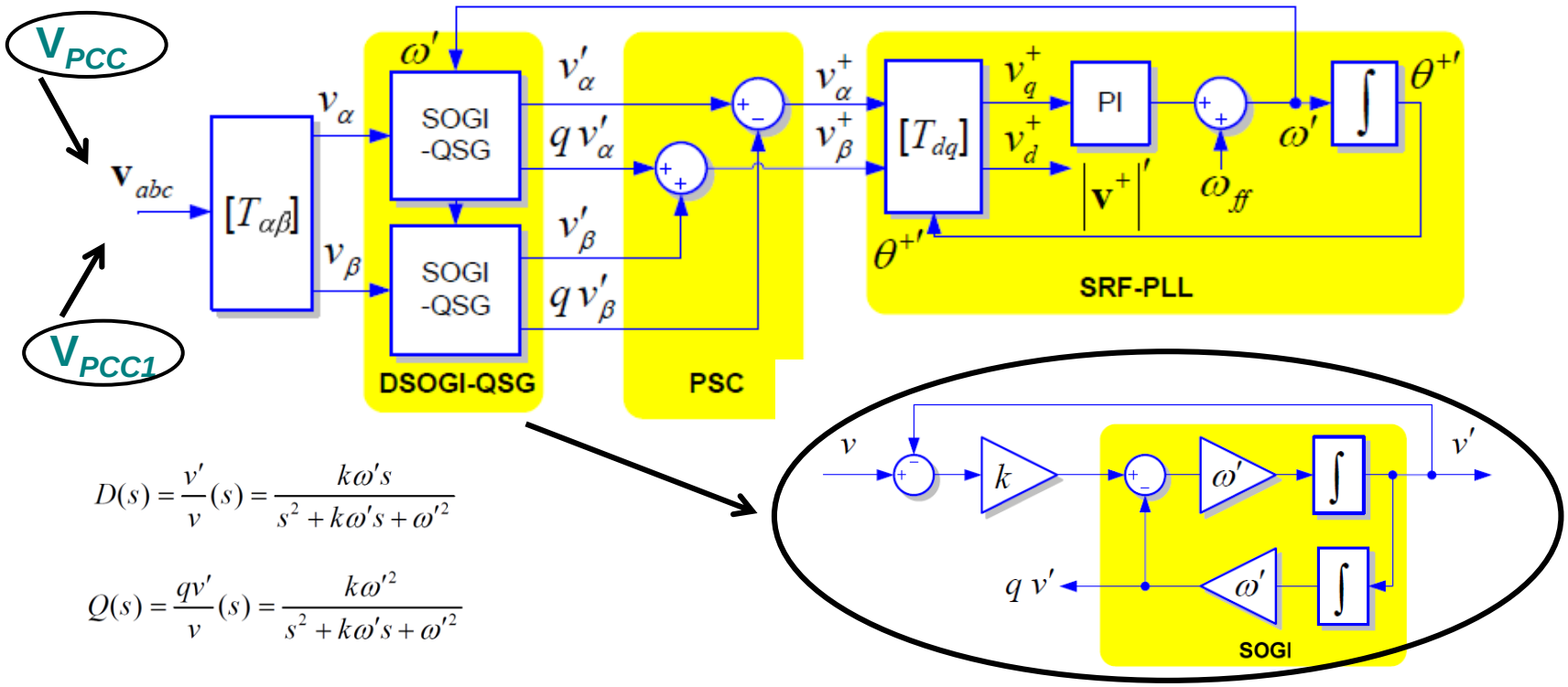

$$D(s) = \frac{v'}{v}(s) = \frac{k\omega' s}{s^2 + k\omega' s + \omega'^2}$$

$$Q(s) = \frac{qv'}{v}(s) = \frac{k\omega'^2}{s^2 + k\omega' s + \omega'^2}$$

- The synchronization system is based on two dual second order generalized integrator DSOGI-PLLs one is used for monitoring V_{PCC} and the other for V_{PCC1}.
- The SOGI-PLL is based on frequency adaptive quadrature-signals generation by means of the Second-Order Generalized Integrator (SOGI) filter employed as a sequence detector in order to extract the positive sequence of the fundamental frequency (FFPS).
- The FFPS is supplied to the PLL to extract the information about its phase and amplitude.

Resonant Controllers

- The Resonant controllers in a stationary reference frame provide a significant advantage compared to the use of PI controllers working in a d,q synchronous reference frame when controlling unbalanced sinusoidal currents.
- Resonant controllers do not require the implementation of decoupling networks neither sequence control as such controllers are able to control both positive and negative sequence components with a single resonant controller.

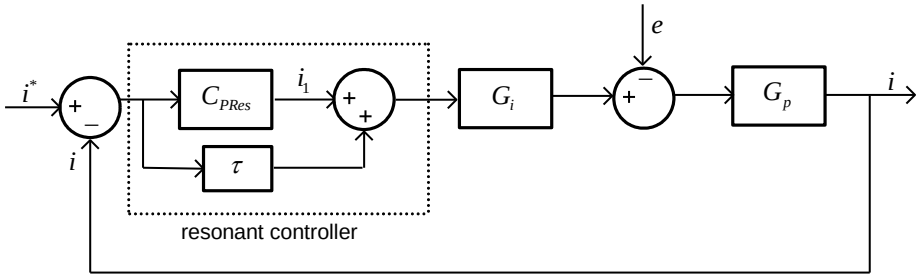

$$P + \mathrm{Re}\,sonant(s) = k_p + k_i \frac{s}{s^2 + \omega^2}$$

$$\tau(s) = \sum_h k_{ih} \frac{s}{s^2 + (h\omega)^2}$$

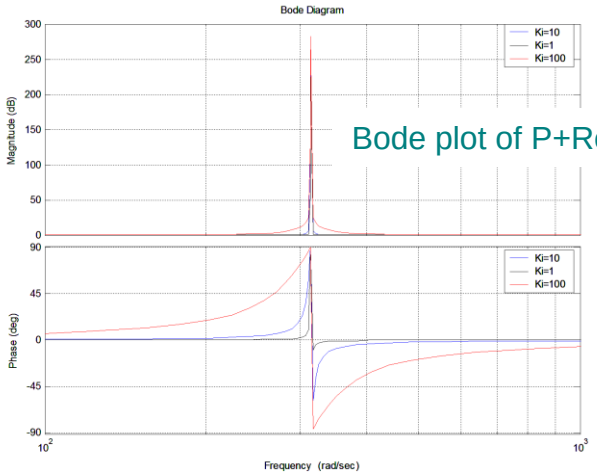

Bode plot of P+Resonant controller

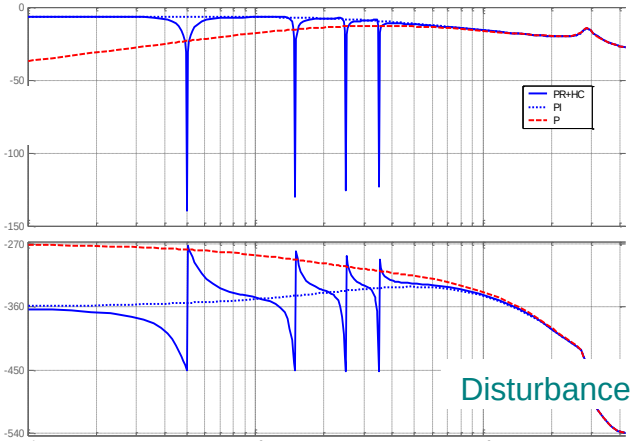

Disturbance rejection

Results: unbalanced currents

- The performances of the voltage and current control are tested in case of an unbalanced load consisting of a 0.4 pu decrement related just to one phase.

- It can be noticed that the voltage control is not affected by the currents imbalance and that the current tracking capability is guaranteed even if $i_{1\alpha}^*$ and $i_{1\beta}^*$ are different each other

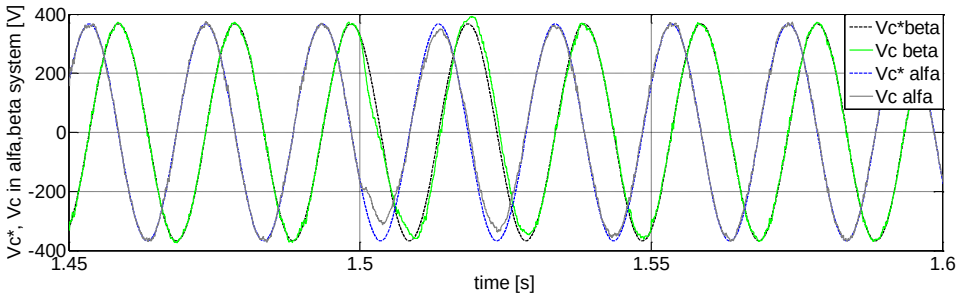

a)

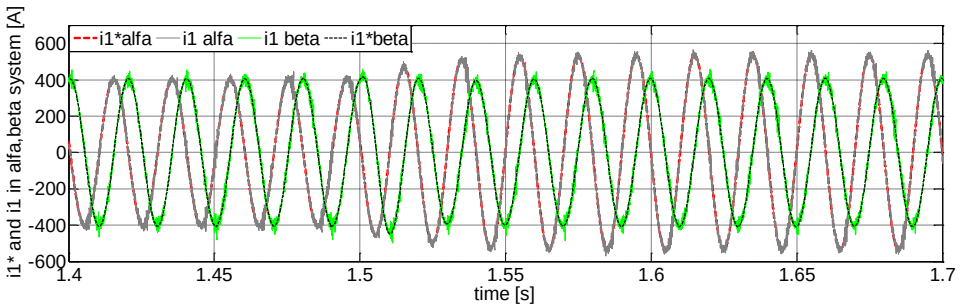

b)

Performance of the control system in case a load imbalance of 0.4 pu occurring at t=1.5 s: a) capacitor voltage control; b) i1 current control.

Results: unbalanced currents

- The grid-forming converter behavior has been compared in case of replacement with standard PIs (in a *d-q* rotating reference frame).

- No negligible voltage error occurs when the load imbalance is introduced and this error is after propagated in the rest of the system.

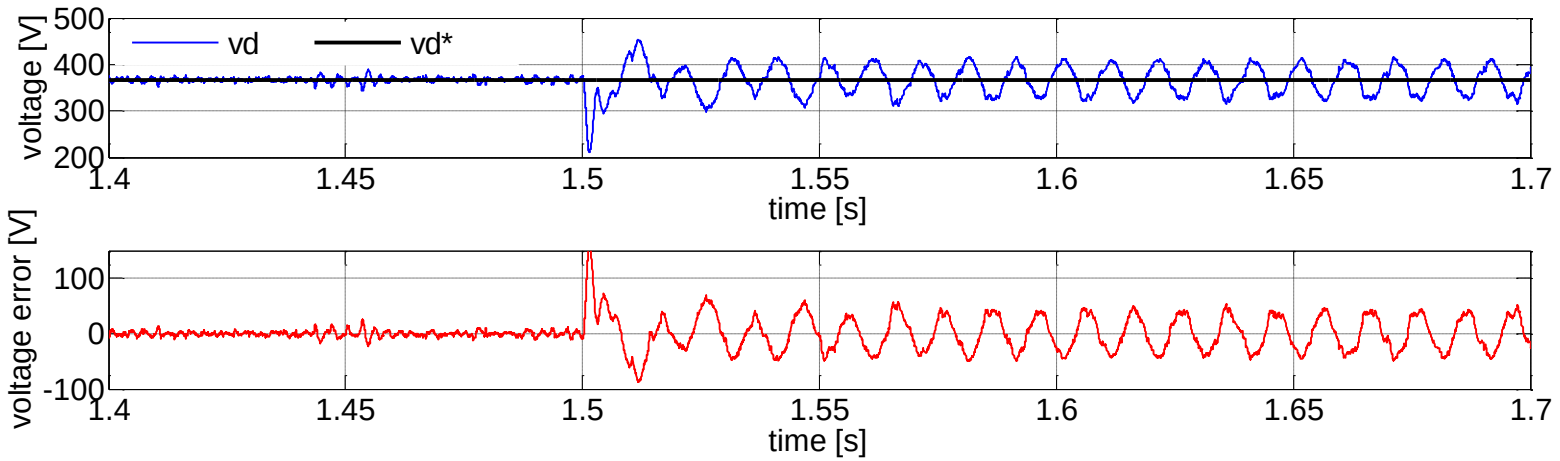

d-axis capacitor voltage and d-axis voltage error in case of PI controllers (instead of P+Resonant controllers) and a load imbalance of 0.4 pu occurring at t=1.5 s

Results: insertion of a grid-feeding converter

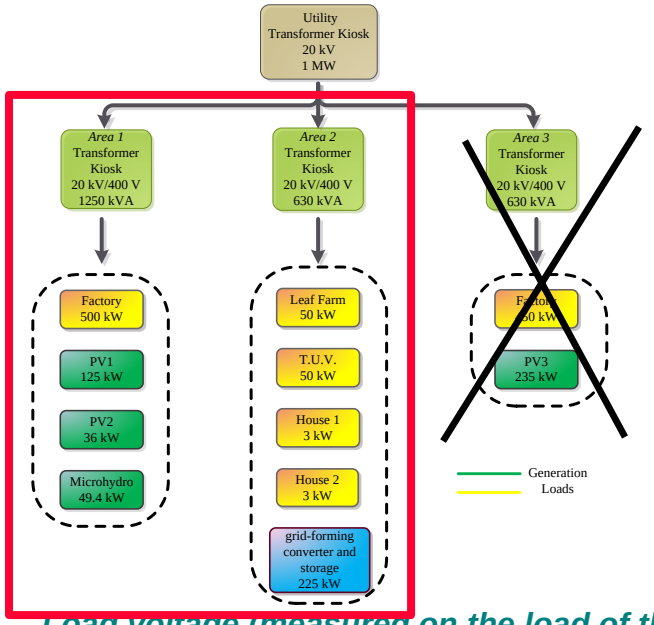

Load voltage (measured on the load of the Area 2) in case part of the Area 1 load is inserted at t=0.5 s and in case of PV1 insertion at t=0.75 s

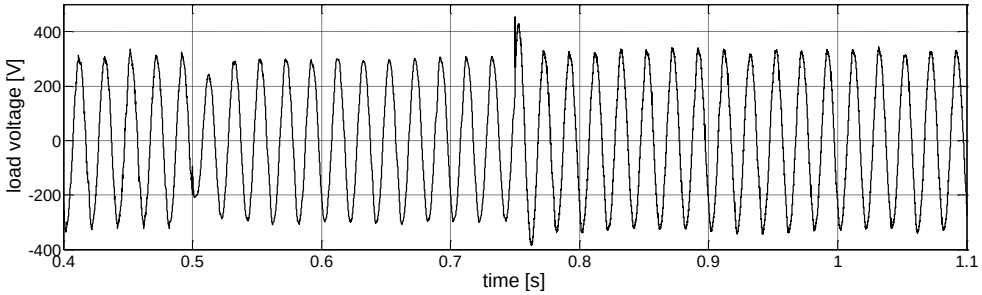

- In the last case the interaction of the grid-forming converter with other DPGS is investigated.
- At t=0 the system operates only with the grid-forming converter supplying the loads of the *Area 2*. At t=0.5 a portion of the loads connected to the *Area 1* is enabled and finally at t=0.75 s the plant PV1 is activated.
- The plant PV1 is modelled considering that its inverter is grid-feeding and it is injecting a power equal to 125 kW into the microgrid (only current control).

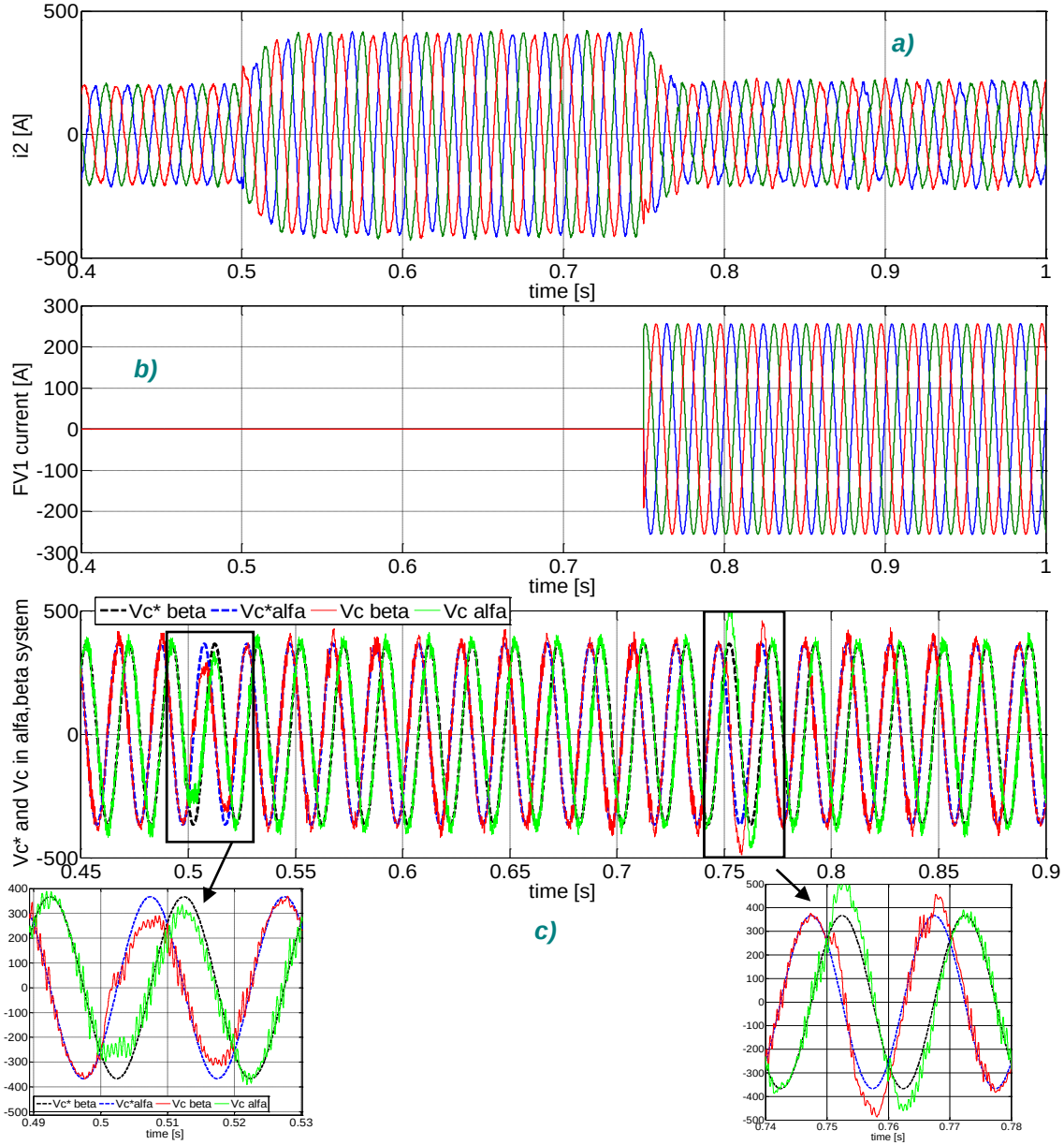

Performance of the system in case part of the Area 2 loads is inserted at t=0.5 s and then at t=0.75 s:

a) i2 provided by the grid-forming converter to the microgrid;

b) current injected by the photovoltaic plant PV1 (grid-feeding converter);

c) zoom of voltage around the transient states.

IN CONCLUSION IT IS DEMONSTRATED THAT RESONANT CONTROLLERS PROVIDE OPTIMAL VOLTAGE CONTROL OF THE GRID-FORMING CONVERTER AT STEADY STATE AND IN CASE OF LOAD INSERTIONS AND TRANSIENT STATES DUE TO THE INSERTION OF OTHER POWER GENERATORS INTO THE MICROGRID BUT THE LOADS CAN BE AFFECTED BY OVERVOLTAGES OR UNDERVOLTAGES IN THE ABSENCE OF A PROPER POWER MANAGEMENT STRATEGY.

Power Management Strategy: the Droop Control

Active power

$$P = \left(\frac{EV}{Z}\cos\phi - \frac{V^2}{Z}\right)\cos\theta + \frac{EV}{Z}\sin\phi\sin\theta$$

Reactive power

$$Q = \left(\frac{EV}{Z}\cos\phi - \frac{V^2}{Z}\right)\sin\theta + \frac{EV}{Z}\sin\phi\cos\theta$$

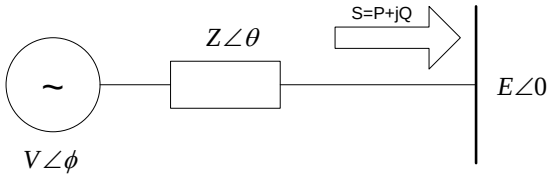

- V is the amplitude of the converter output voltage;
- *E* is the amplitude of the voltage at the point of the connection with the grid;
- Φ is the converter voltage angle;
- *Z* and are the magnitude and the phase of the line impedance.

Assuming that the output impedance is purely inductive and the angle Φ is small the amplitude and the frequency of the control voltage can be expressed as it follows:

$$P = \frac{EV}{X}\sin\phi \approx \frac{EV}{X}\phi$$

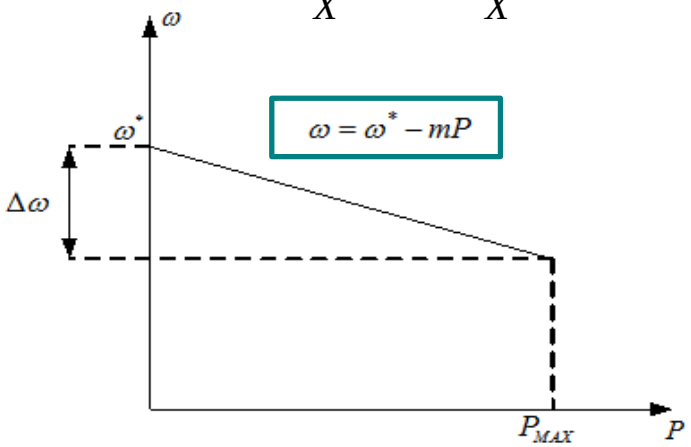

$$Q = \frac{EV}{X}\cos\phi - \frac{E^2}{X} \approx \frac{E}{X}(V - E)$$

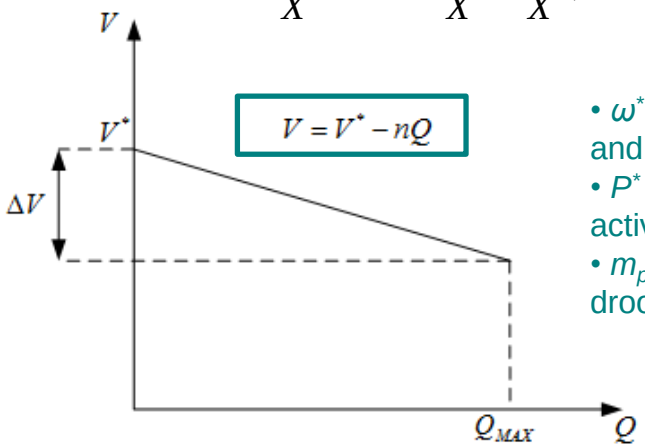

- ω^* and V^* are the rated frequency and voltage;
- P^* and Q^* are the set points for active and reactive power;
- m_p and n_q are the proportional droop coefficients.

rosaanna.mastromauro@poliba.it

Power Management Strategy: the Droop Control

In case of a low voltage micro-grid the **line resistance** cannot be neglected.

Active power

$$P = \frac{E}{X}(V - E) \Rightarrow V = V^* - n(P - P^*)$$

Reactive power

$$Q = \frac{EV}{X}\phi \Rightarrow \omega = \omega^* - m(Q - Q^*)$$

Transformation matrix *T*

$$\begin{bmatrix} P_C \\ Q_C \end{bmatrix} = Z \begin{bmatrix} \sin\theta & -\cos\theta \\ \cos\theta & \sin\theta \end{bmatrix} \begin{bmatrix} P \\ Q \end{bmatrix}$$

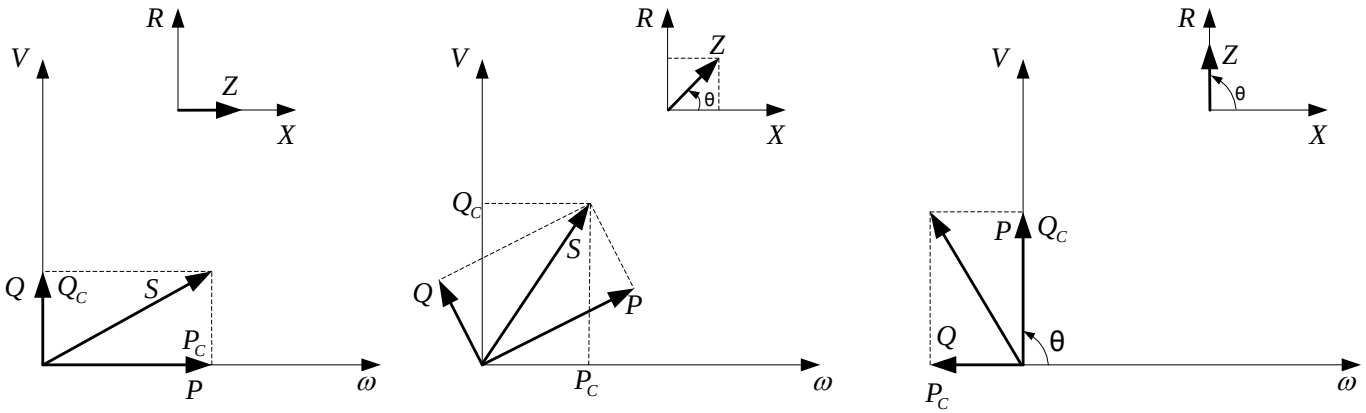

(a) (b) (c)

rosaanna.mastromauro@poliba.it

Droop Control

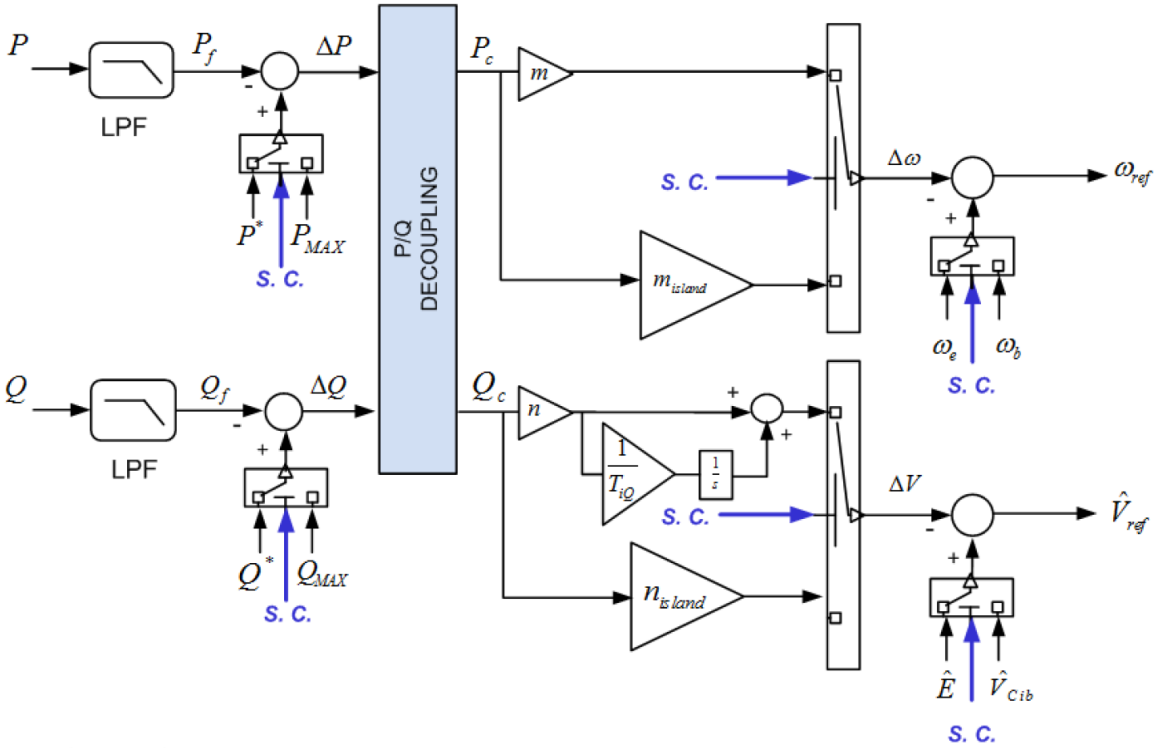

Power Control in Grid-Connected Operation Mode

$$\hat{V} = \hat{E} - n\left[(Q - Q^*) + \frac{1}{T_{iq}}\int_{-\infty}^{t}(Q - Q^*)dt\right]$$

$$\omega = \omega^* - m(P - P^*)$$

Power Control in Stand-Alone Operation Mode

$$\omega = \omega_b - m_{island}(P - P_{MAX})$$

$$\hat{V} = \hat{V}_{Cb} - n_{island}(Q - Q_{MAX})$$

rosaanna.mastromauro@poliba.it

Results

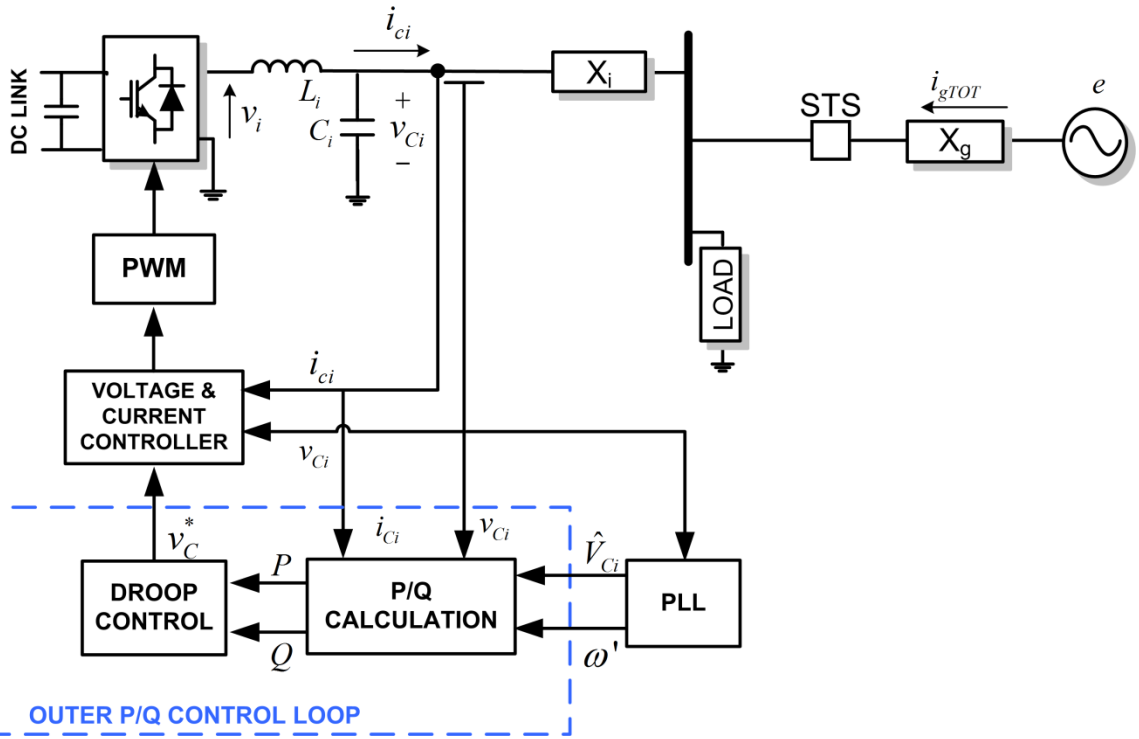

- Normal operation mode
- Short duration interruption
- Outage of an inverter
- Voltage sag

rosaanna.mastromauro@poliba.it

Results: Normal Operation Mode

Active and reactive powers of inverters

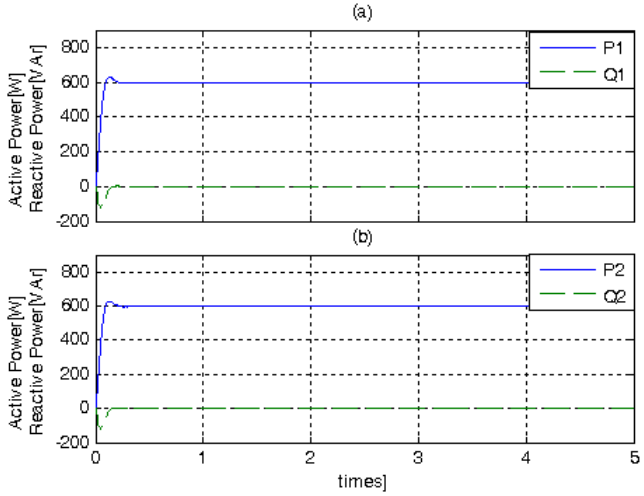

output current

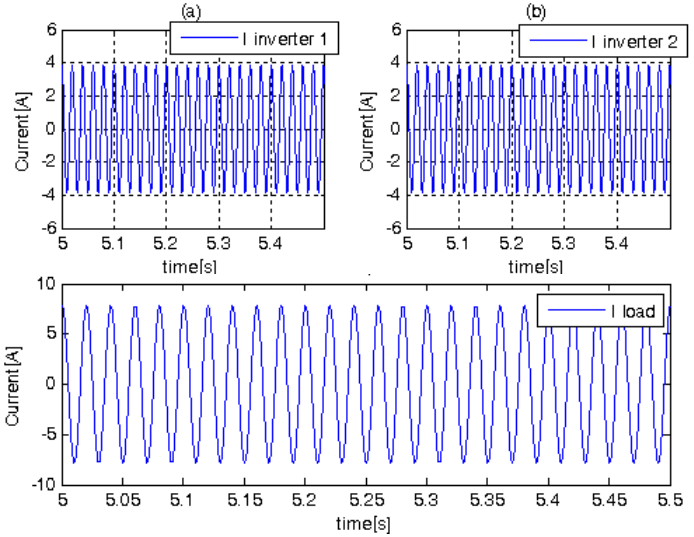

Tested regards the grid-connected operation mode. With the droop control, the inverters can share power (active and reactive power) required by the load without using a communication system.

Grid voltage and inverters output voltage

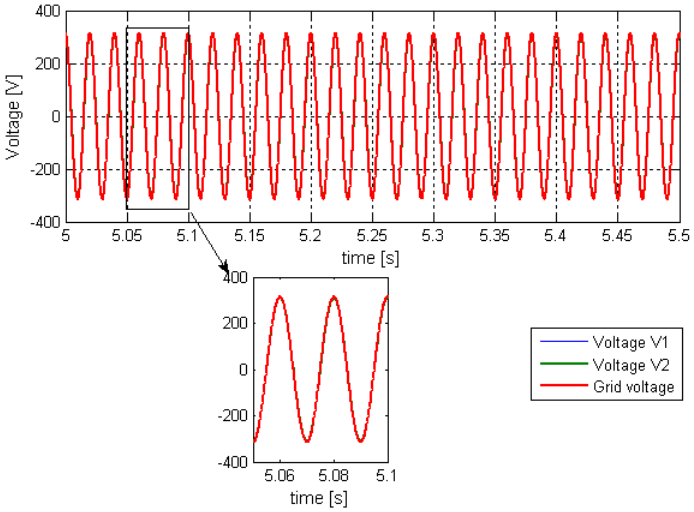

Voltage amplitude and Frequency

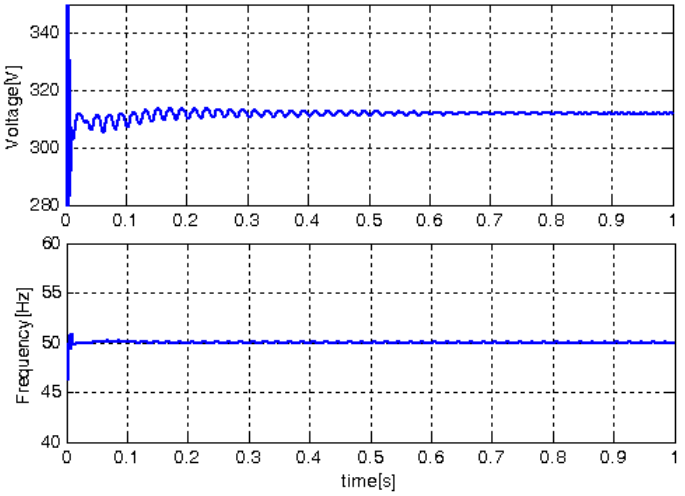

Results: Short Duration Grid Interruption

Active and reactive power outputs of the DPGS system

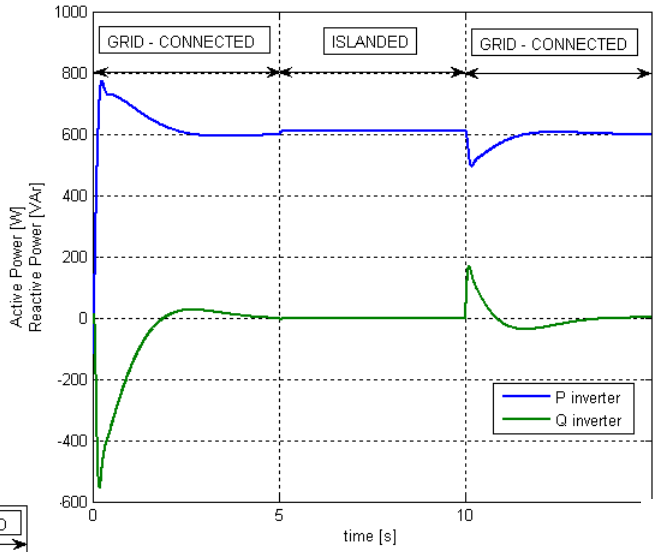

Frequency of the converter

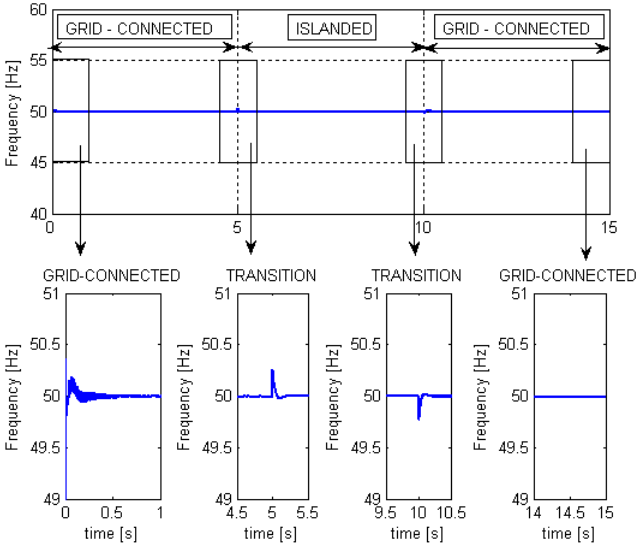

A short duration grid interruption occurs at time t=5s and the DPGS system switches from grid-connected to islanded mode operation. At t=10s the micro-grid switches from islanded to grid-connected mode.

Voltage of the converter

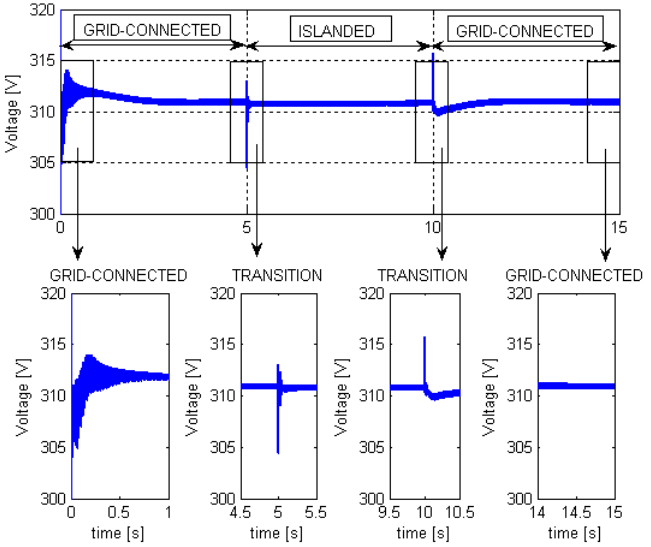

Results: Outage of an Inverter

Active and reactive power

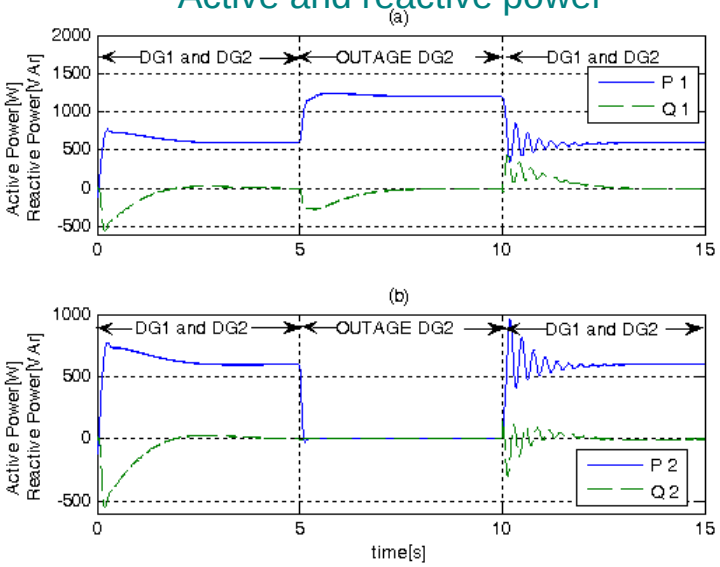

Frequency on common bus

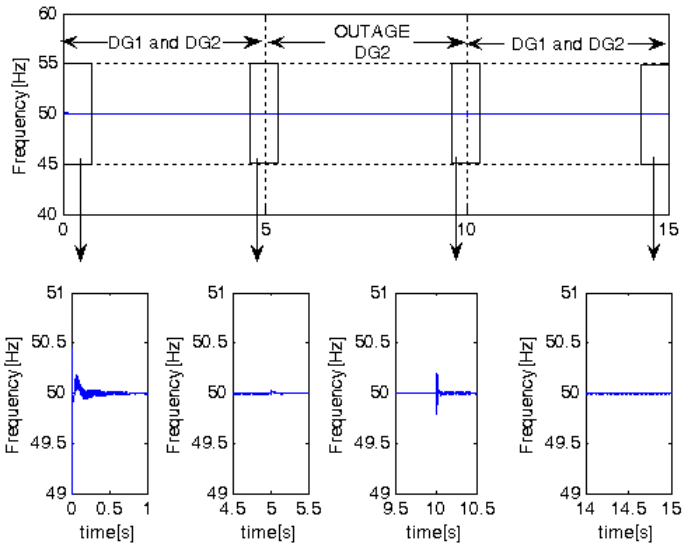

From t=5s to time t=10s the inverter 2 is affected by a disservice, while the inverter 1 has to cope with the total load power demand

Voltage on common bus

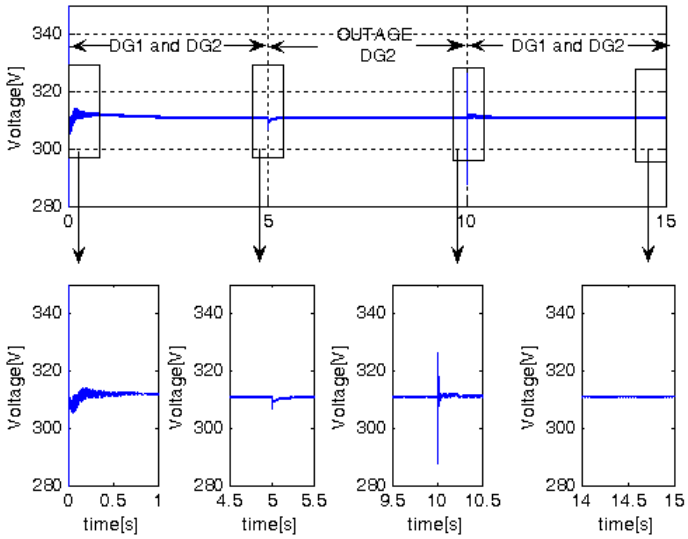

Results: Voltage Sags

Active and reactive power

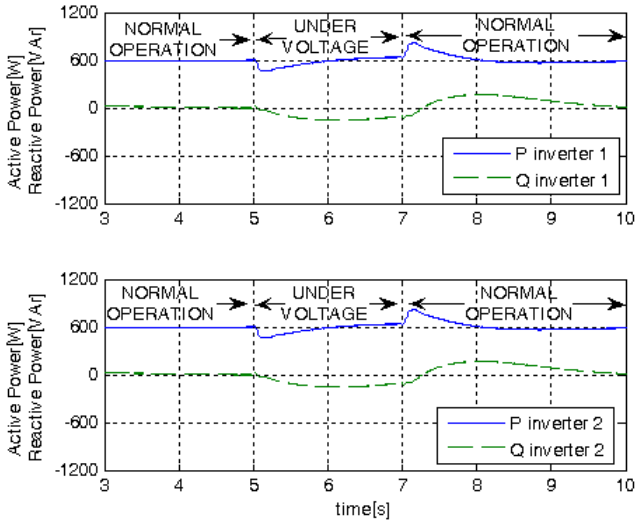

Frequency on common bus

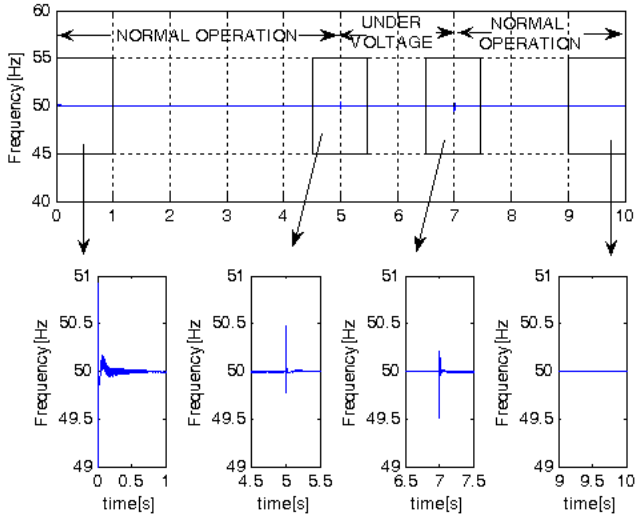

During voltage sag, the inverters are able to share active and reactive power required by the load following the references set by the droop control algorithm.

Droop control maintains the frequency constant on common bus, but the voltage amplitude decreases because references in the droop control come from the PLL.

Voltage on common bus

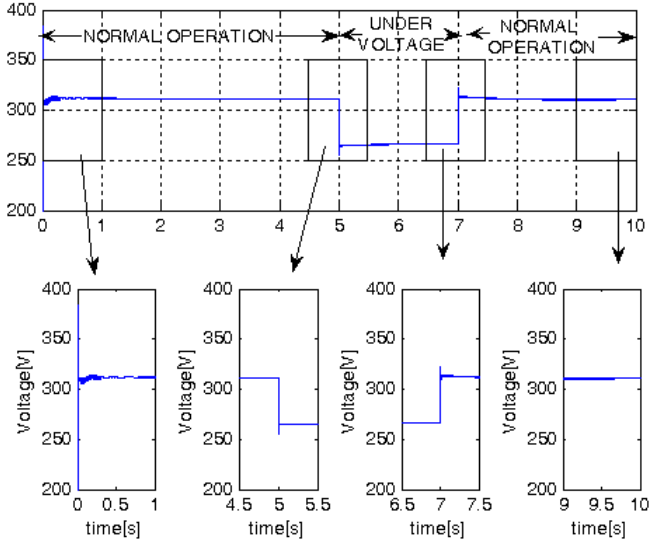

Experimental Setup

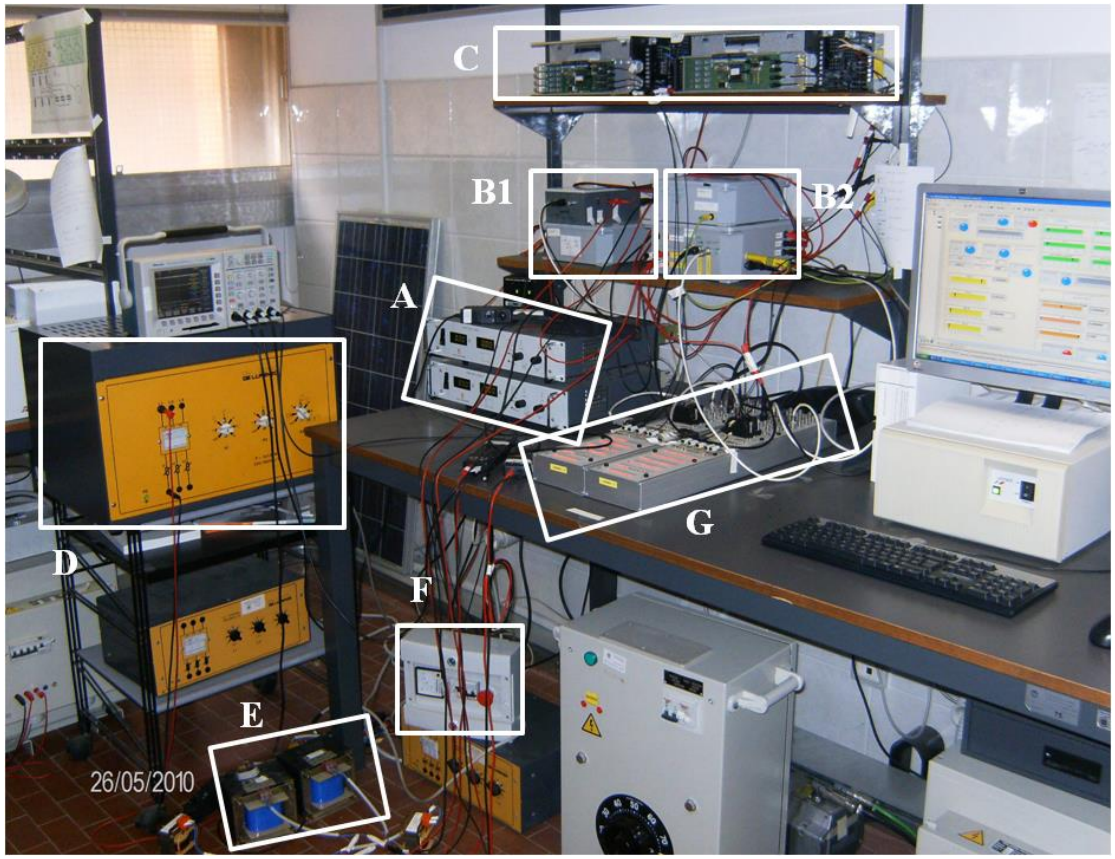

The laboratory setup:
A - two DC power supplies;
B1- filter 1 + current and voltage acquisition boards (system 1);
B2 - filter 2 + current and voltage acquisition boards (system 2);
C - two inverters;
D - load;
E - isolation transformer;
F - static transfer switch (STS);
G - two 1103 dSpace boards

rosaanna.mastromauro@poliba.it

Experimental Results: Outage of an Inverter

transition from grid-connected to stand-alone operation

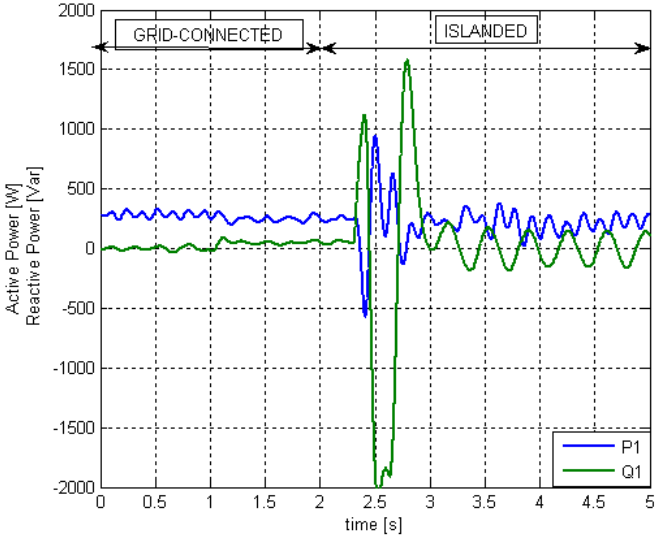

Inverters currents (CH3 and CH4), grid-voltage (CH1) and voltage at the common bus (CH2) considering grid-connected operation mode and inverter 1 is affected by a disservice

currents

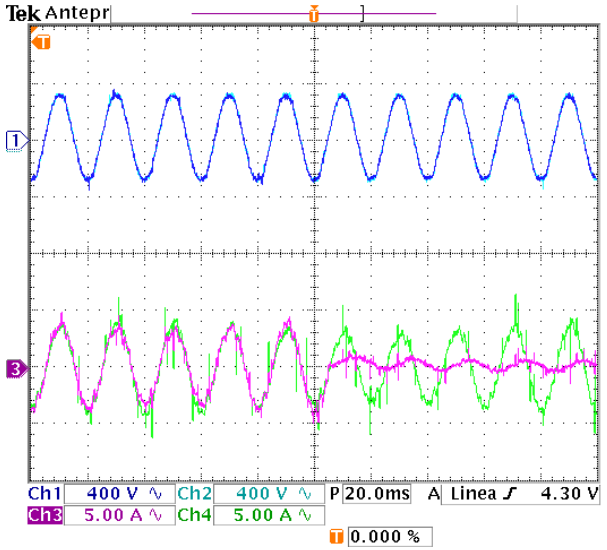

active and reactive power

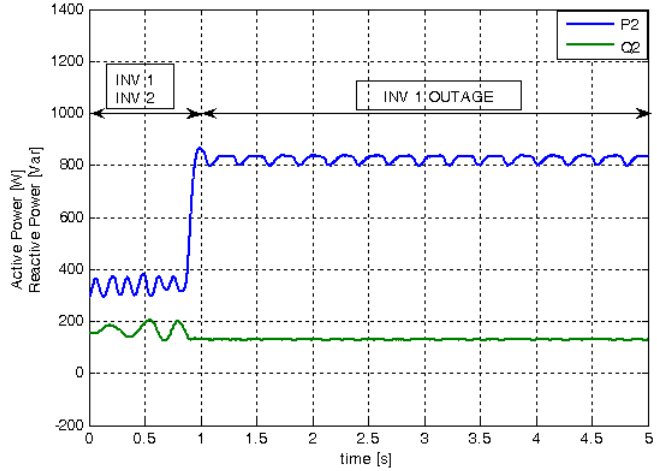

frequency

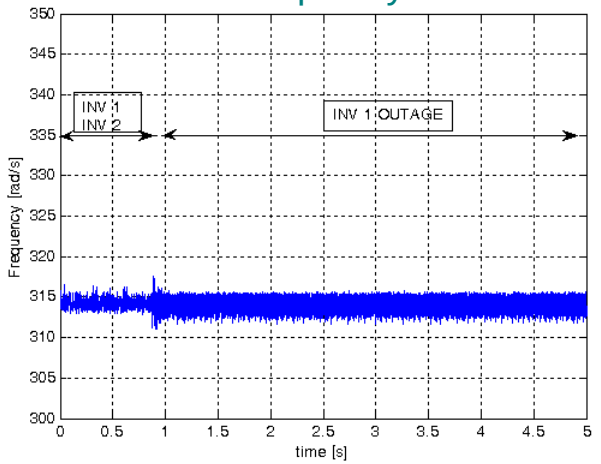

DC MICROGRIDS: SINGLE-STAR BRIDGE CELLS (SSBC) MODULAR MULTILEVEL CASCADE CONVERTER (MMCC) CONVERTER FOR DC MULTIBUS APPLICATIONS

rosaanna.mastromauro@poliba.it

DC Microgrids and AC Microgrids

The actual power system is in AC: the reasons of this choice are several, among them there are the flexible connection to transformers and induction motors and the need to transfer high power for long distances.

Just in some application it is used the DC transmission:

- **Electric traction**

- **Submarine distribution**

- **Industrial drives**

- **Electrochemical applications**

rosaanna.mastromauro@poliba.it

DC Microgrids and AC Microgrids

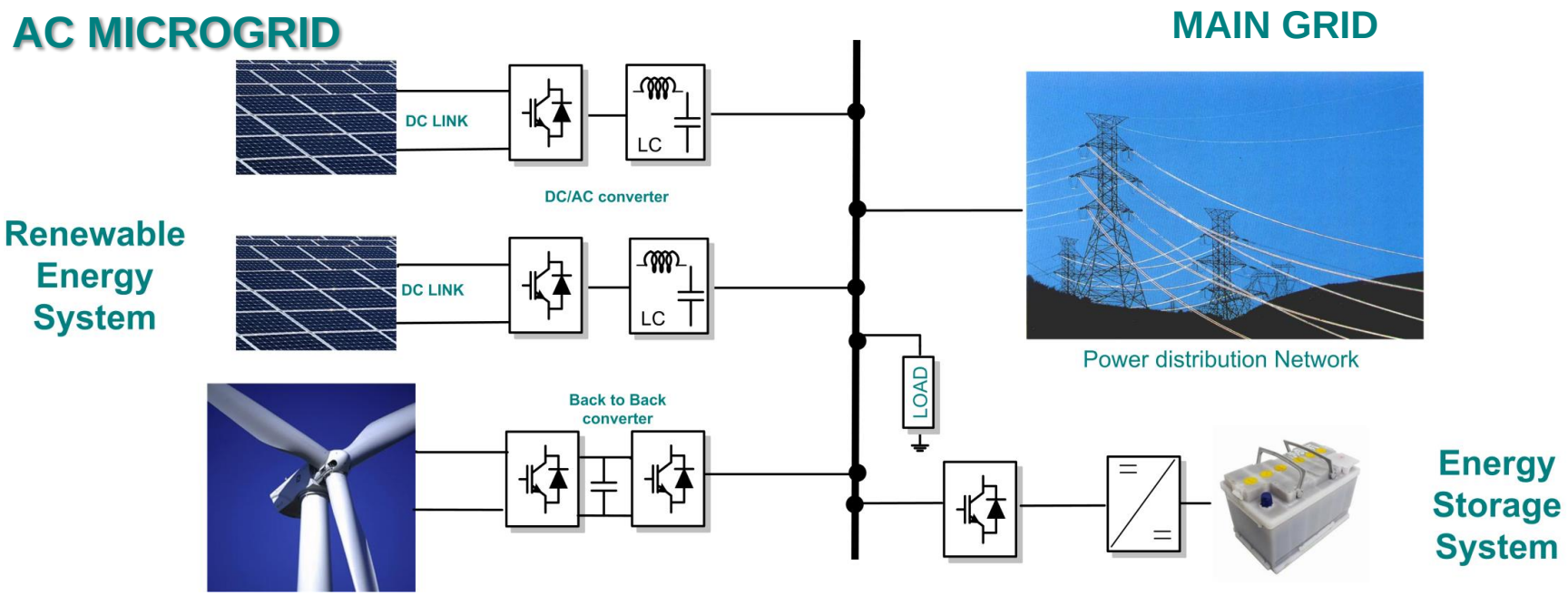

Advantages of DC microgrids
Drawbacks of DC microgrids

- High system efficiency due to one-stage power conversion;
- Need to create DC distribution lines;
- Synchronization with the main grid is not needed (no frequency and/or phase control);
- Protections circuit complexity (no zero-crossing detection);
- Continuous operation mode in case of AC faults due to the storage energy systems included in the DC microgrid;
- Potential instability due to coexistence of different voltage levels.
- Better integration of energy storage and renewable power sources (almost all of them are intrinsically DC)

rosaanna.mastromauro@poliba.it

Configuration of the DC Microgrid with a SSBC MMCC

Main components:

- Distributed generation sources;
- Energy storage systems;
- Critical and non-critical loads.

DC LOAD

The DC Multibus provides:

- Different DC voltage levels
- Redundancy;

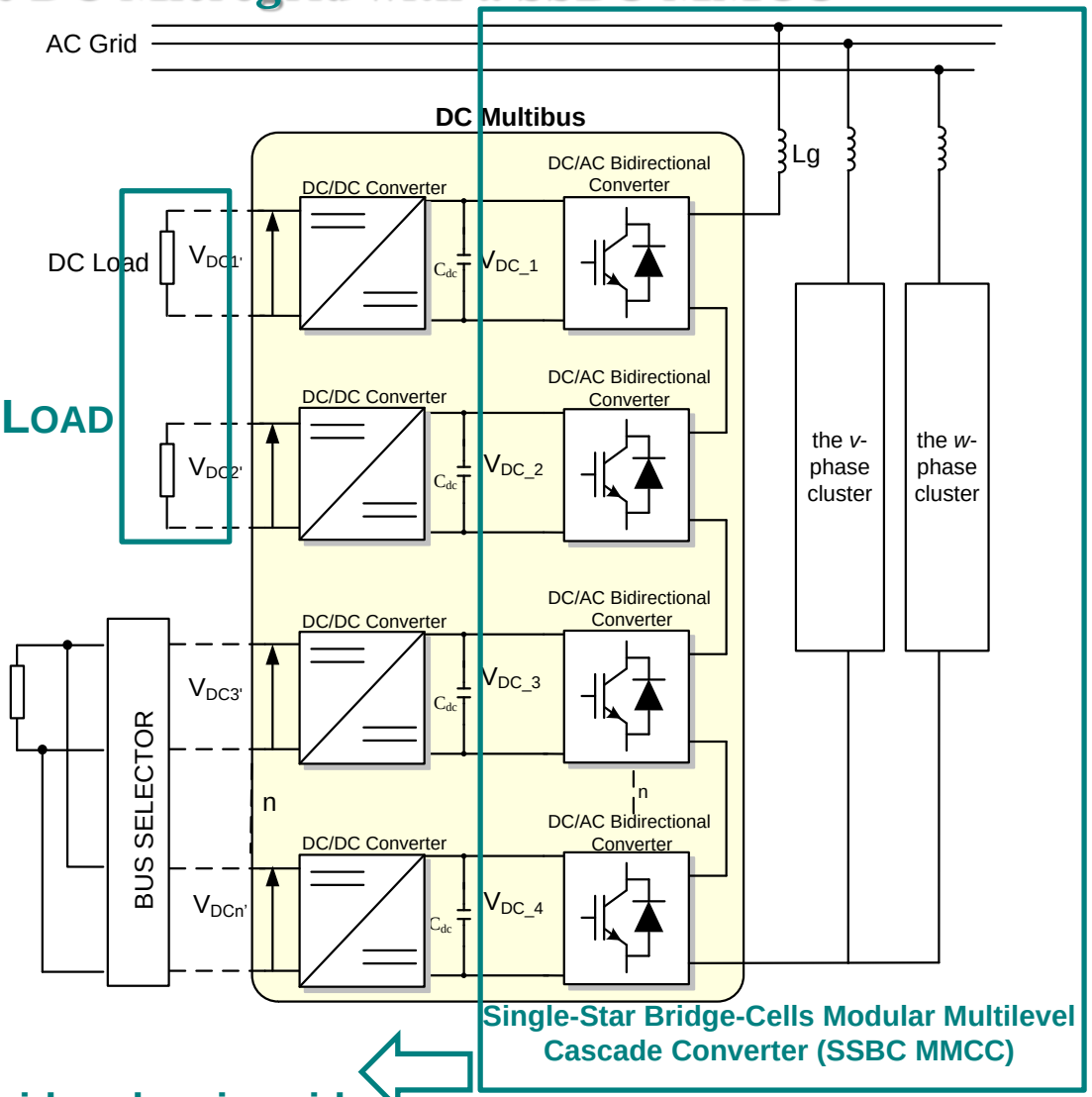

Interface between DC Microgrid and main grid

DC Multibus Selectors

The "Bus Selectors'' chooses which bus energizes each load. The Multibus arrangement with a suitable bus selector can provide continuous power to loads in case of significant damage on one of the DC buses.

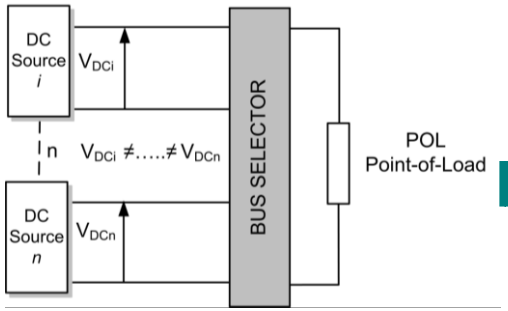

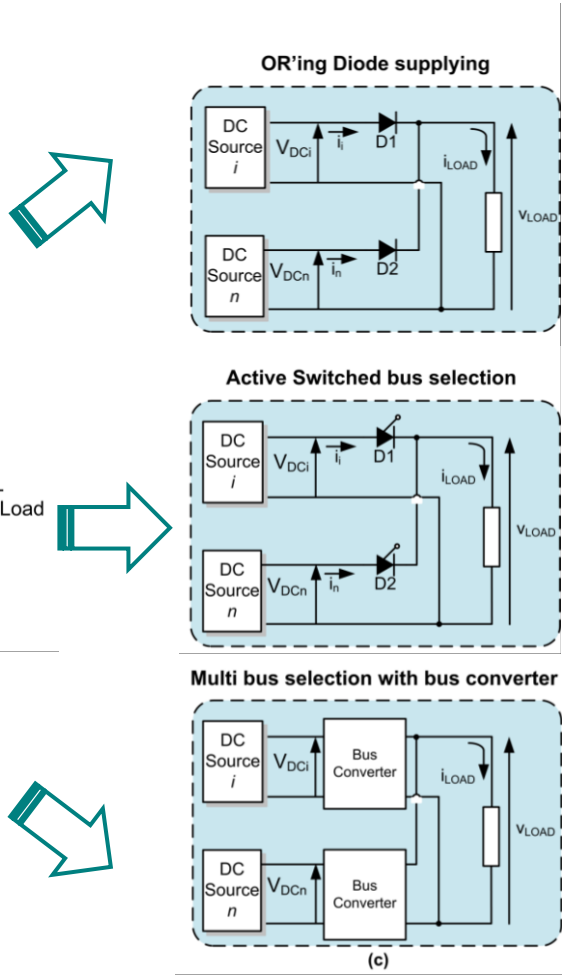

The diode automatically and passively chooses the bus with the highest voltage to supply the load.

The bus selection is realized by a simple control strategy :

If $v_1 \geq v_2 + \delta$ Bus 1
If $v_2 < v_2 + \delta$ Bus 2.

The output of DC/DC converters are connected in parallel in order to supply the load and to ensure the reliability of the system.

AC/DC Interface based on the Single-Star Bridge-Cells (SSBD) Modular Multilevel Cascade Converter (MMCC)

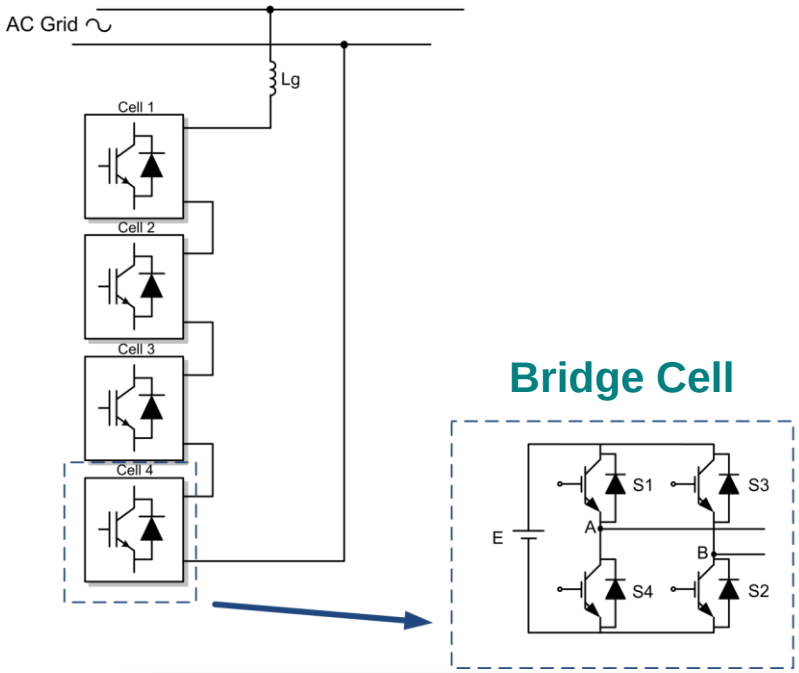

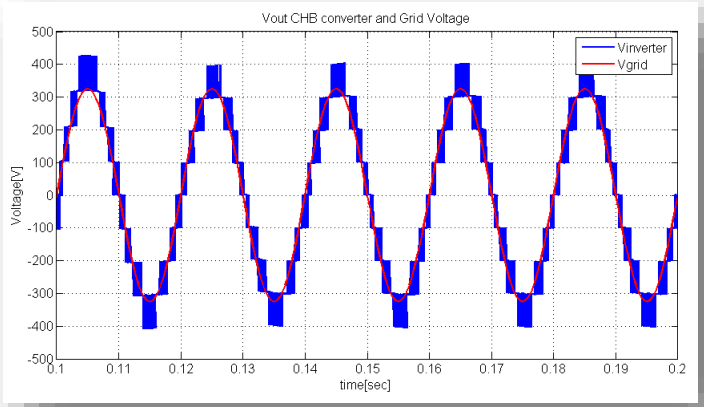

Advantages of SSBC MMCC

- Modularity and reliability;
- High power with high voltages;
- Multiple DC outputs;
- Low harmonic distortion;
- Bi-directional;
- Low frequencies and switching losses;
- Small input filters.

Drawbacks of the SSBC MMCC

- Large numbers of components;
- Control of V_{dc}.

→ **9 levels Voltage**

Control of the single cell of the SSBC MMCC

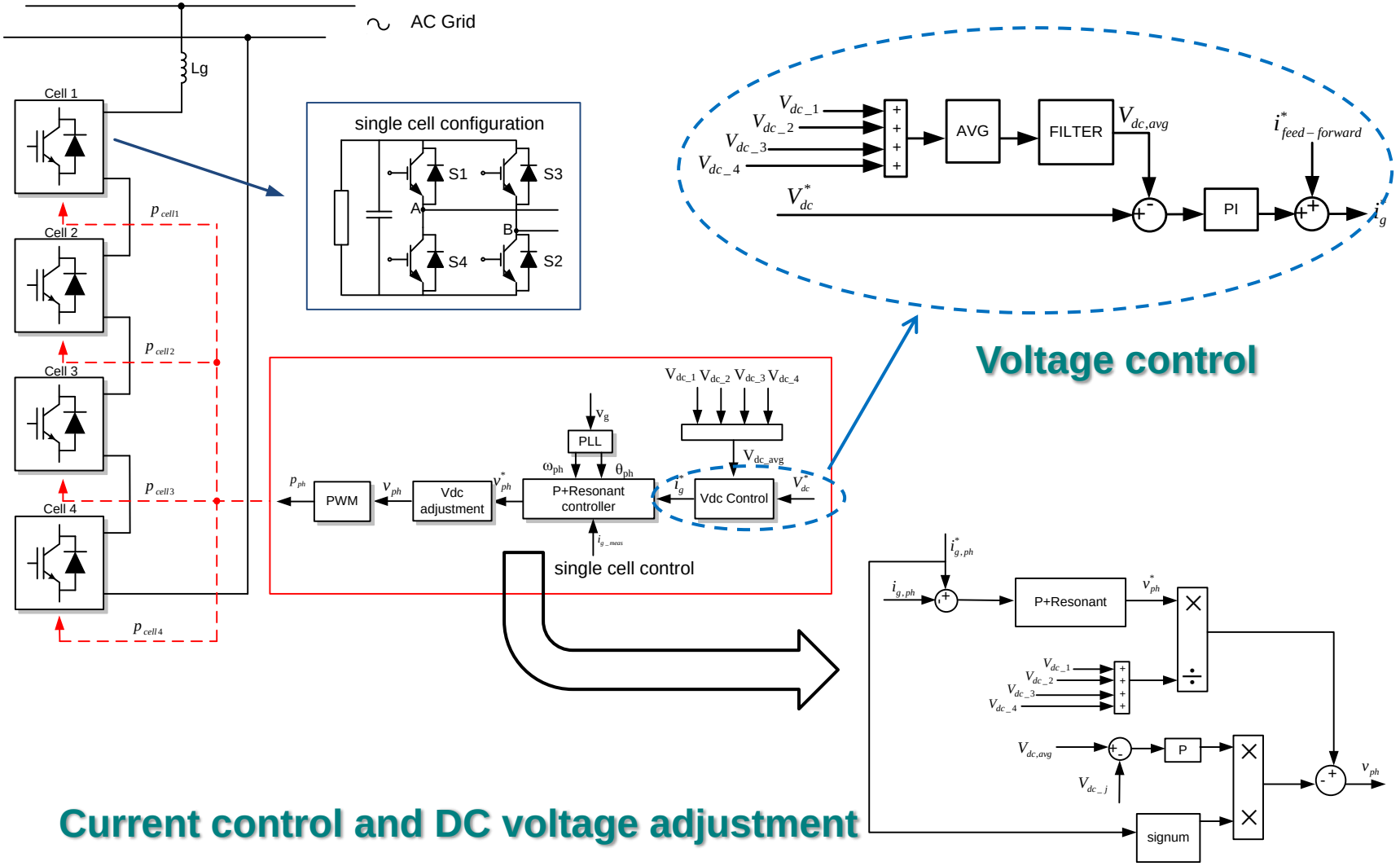

Current control and DC voltage adjustment

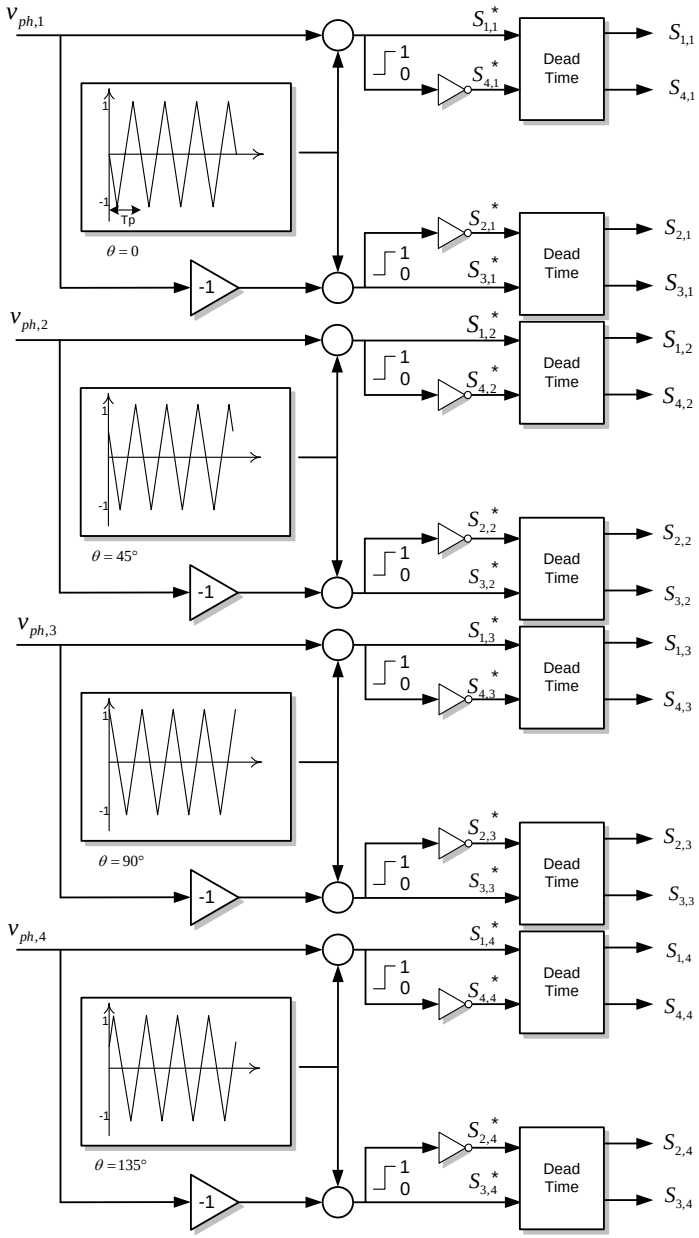

$$\phi_{cr} = \frac{360°}{(m-1)} = 45° \qquad f_{sw} = 1100Hz$$

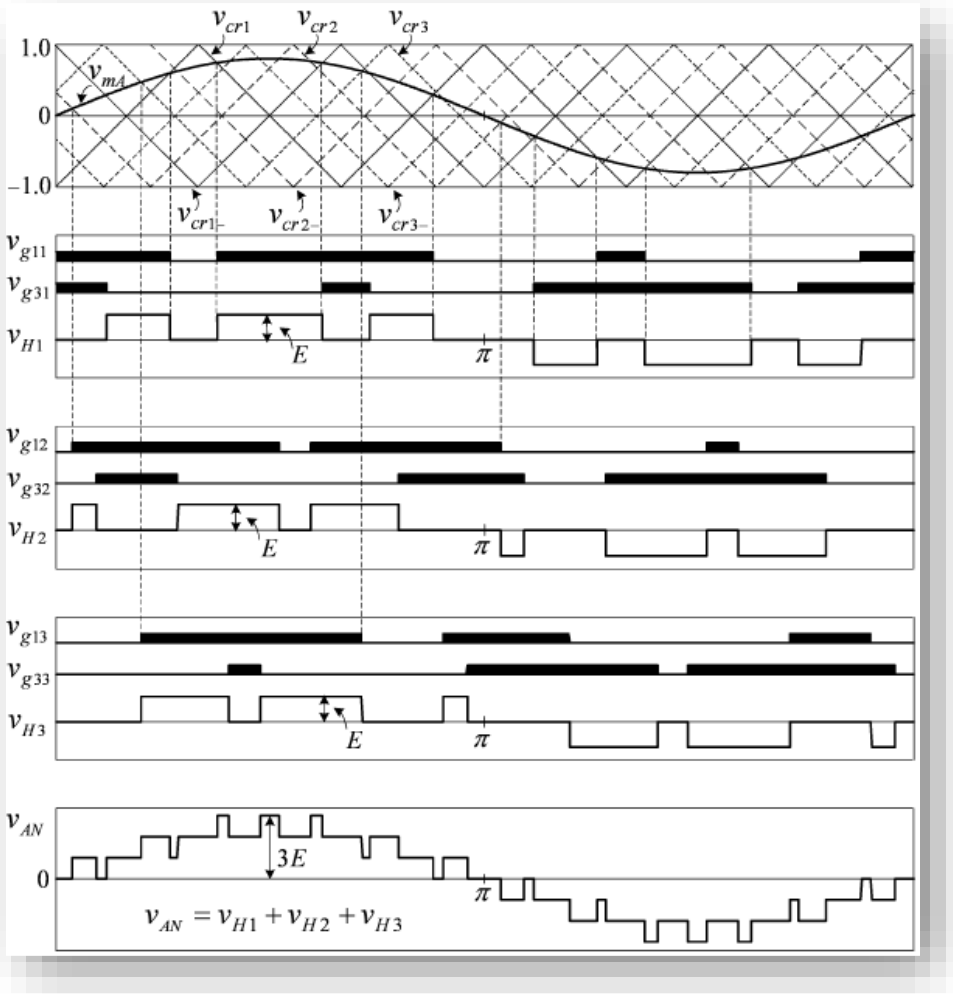

DC Multibus control

DC/DC DAB Converter

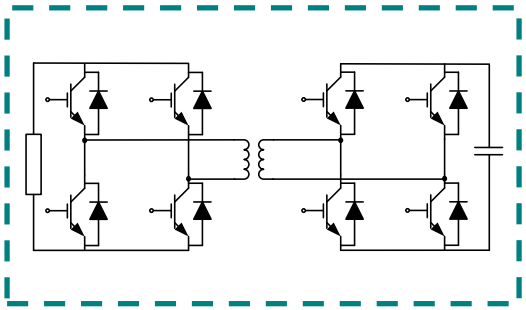

Control of the DAB Converter

DC Multibus with Independent Loads

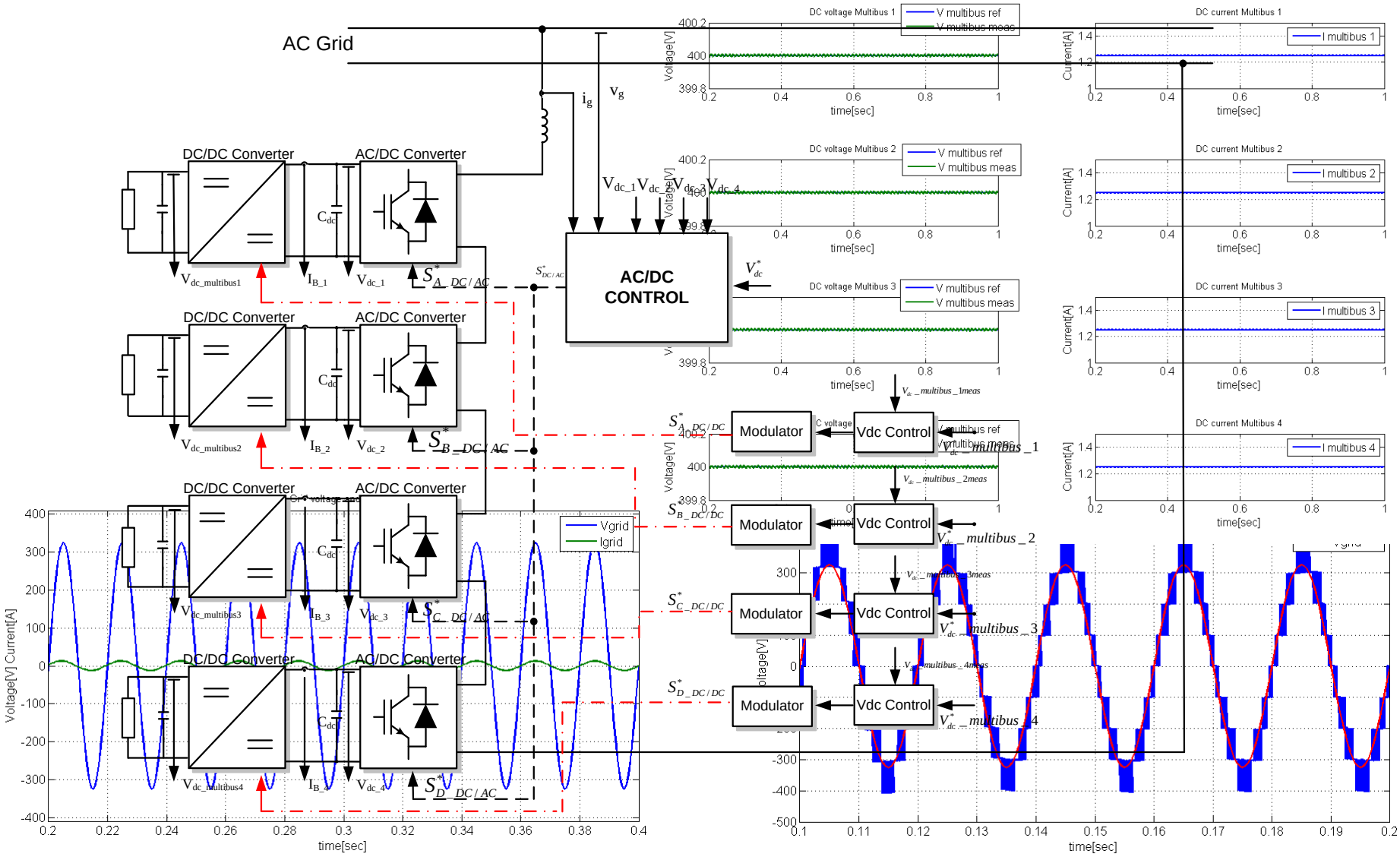

DC Multibus Operating with Different Voltage Levels: 300-400-250V and Load in Parallel

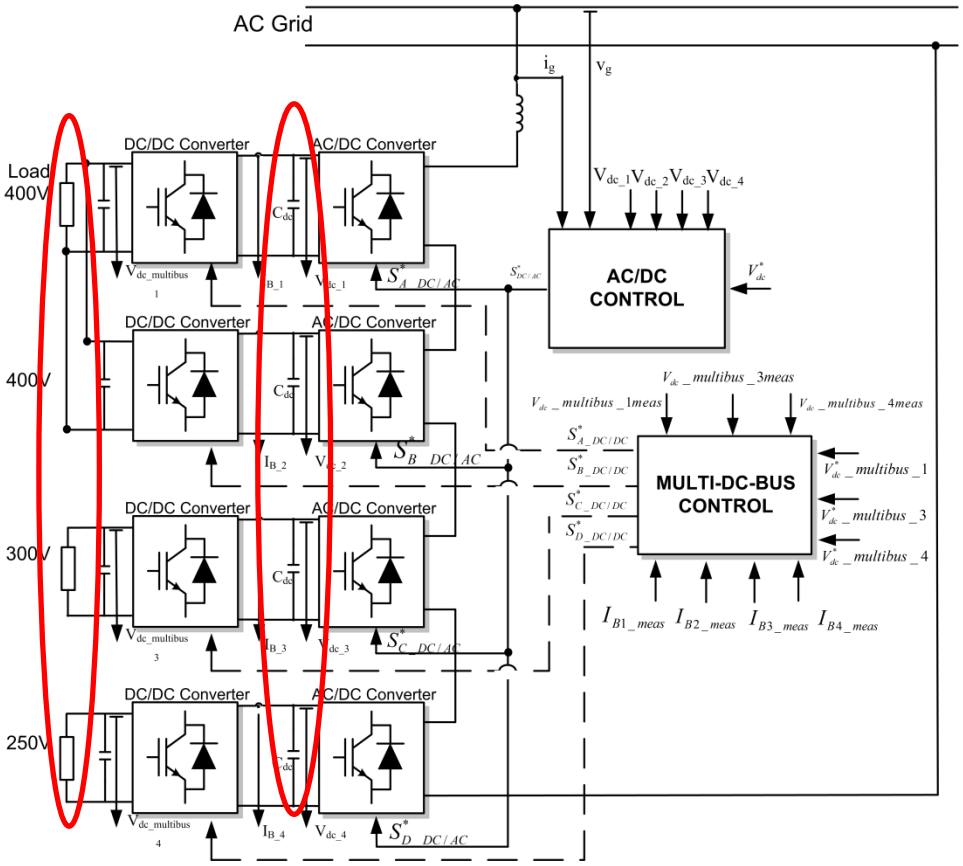

	bus 1	bus 2	bus 3	bus 4
	parallelo a 400V		300V	250V
Load [Ω]	160		180	125
Powera [W]	1000		500	500
Current [A]	2,5		1,66	2

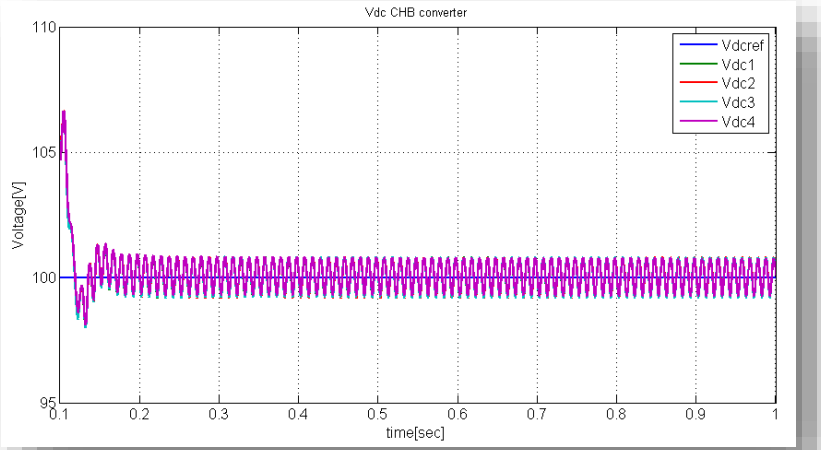

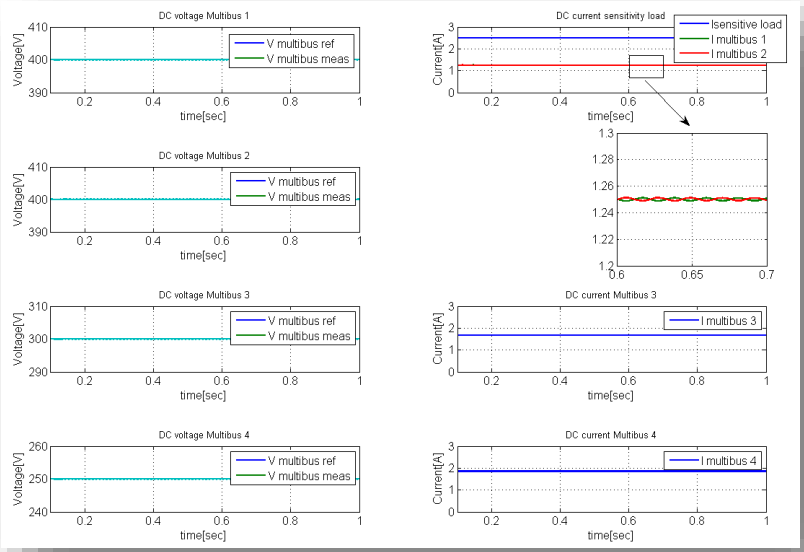

Robustness Analysis: DC Multibus Behavior in the Case of 10% Load Variation for Each Bus

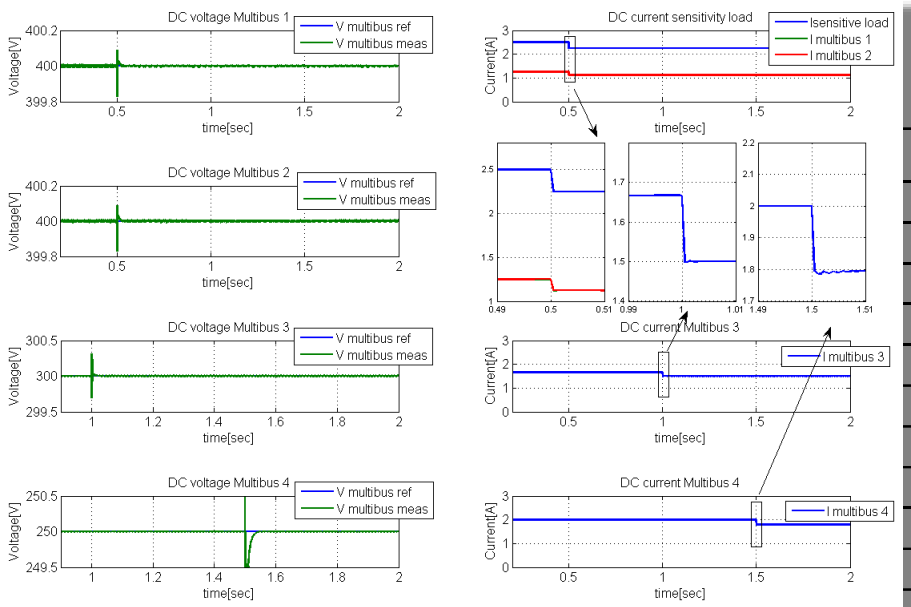

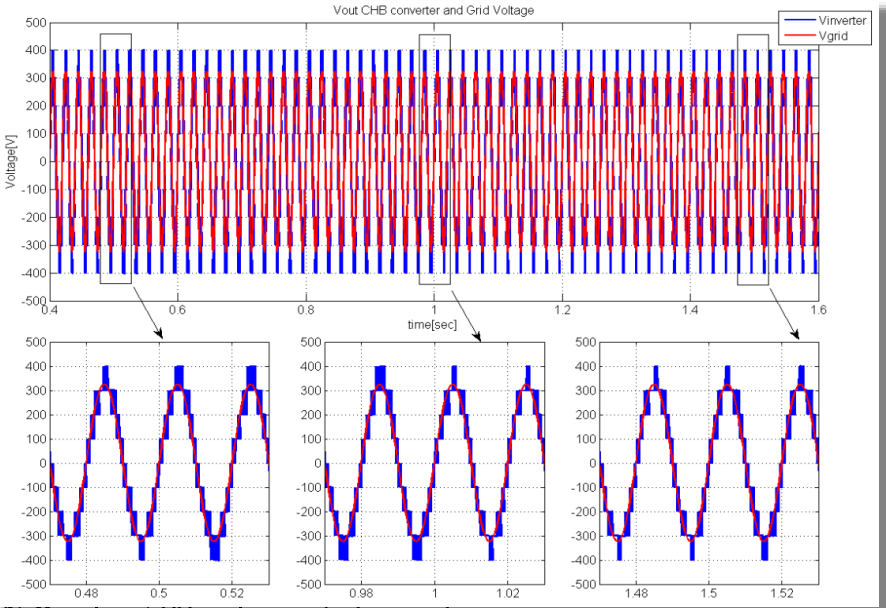

Power[W]	900	450	500
Current[A]	2.25	1.5	2
Load			t=1
Pow			
Curr			

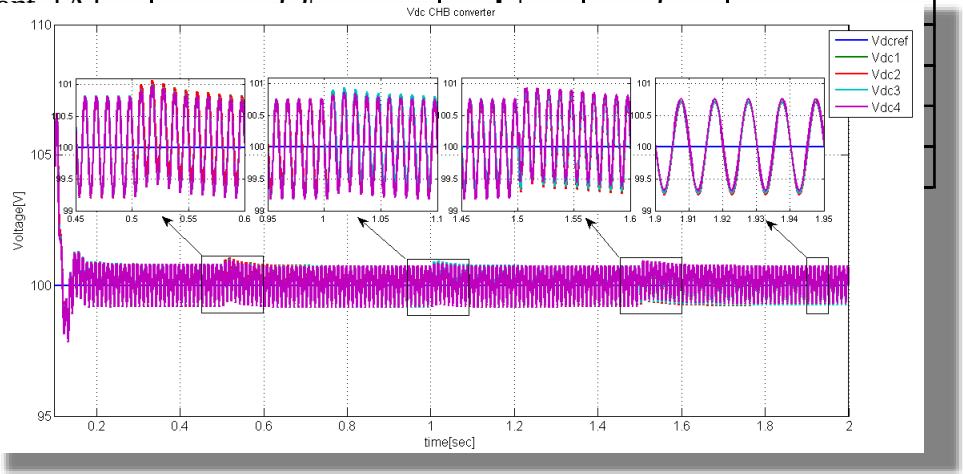

Robustness Analysis: DC Multibus Behavior in the Case of 40% Load Variation

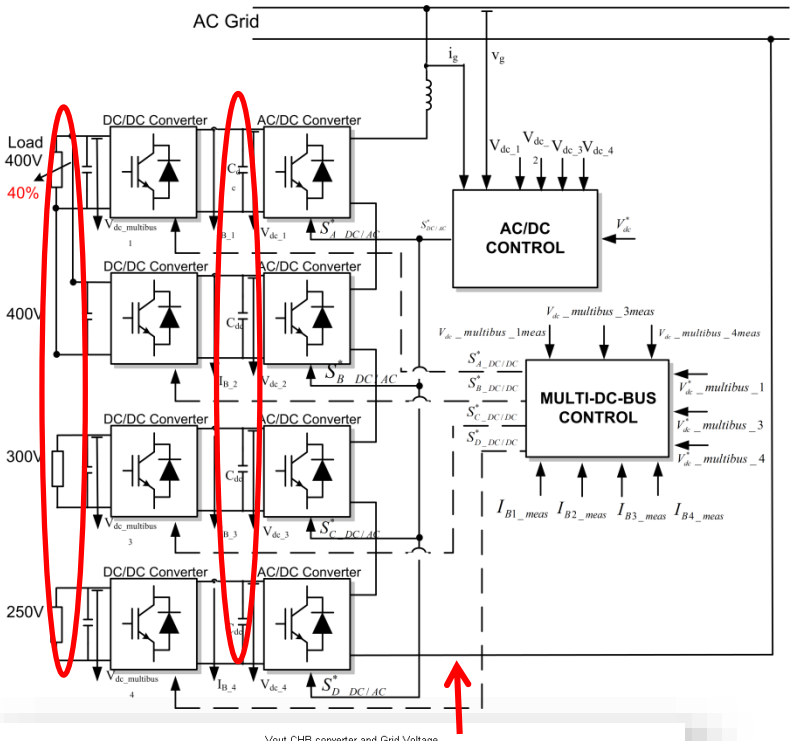

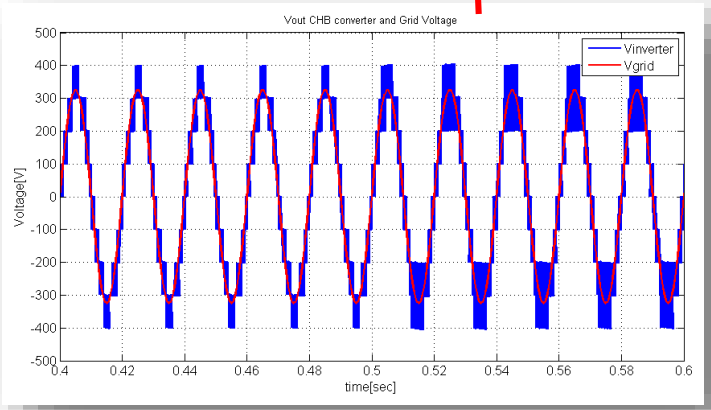

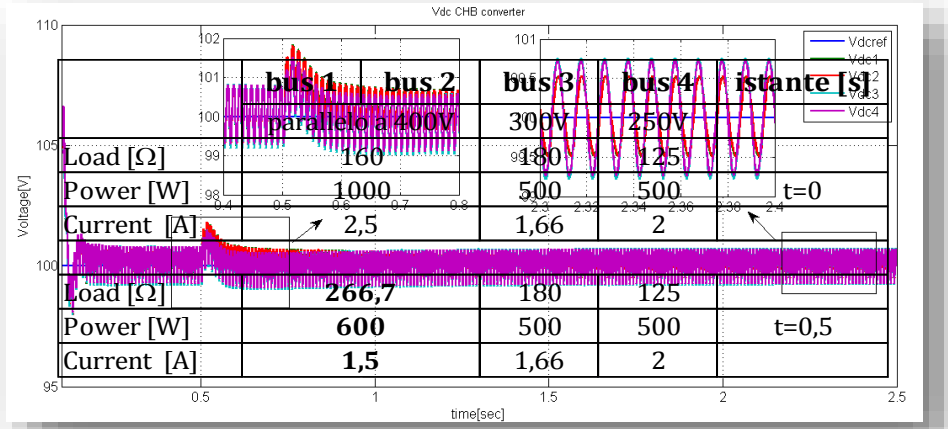

	bus 1	bus 2	bus 3	bus 4	istante [s]
	parallelo a 400V		300V	250V	
Load [Ω]	160		180	125	
Power [W]	1000		500	500	t=0
Current [A]	2,5		1,66	2	
Load [Ω]	**266,7**		180	125	
Power [W]	**600**		500	500	t=0,5
Current [A]	**1,5**		1,66	2	

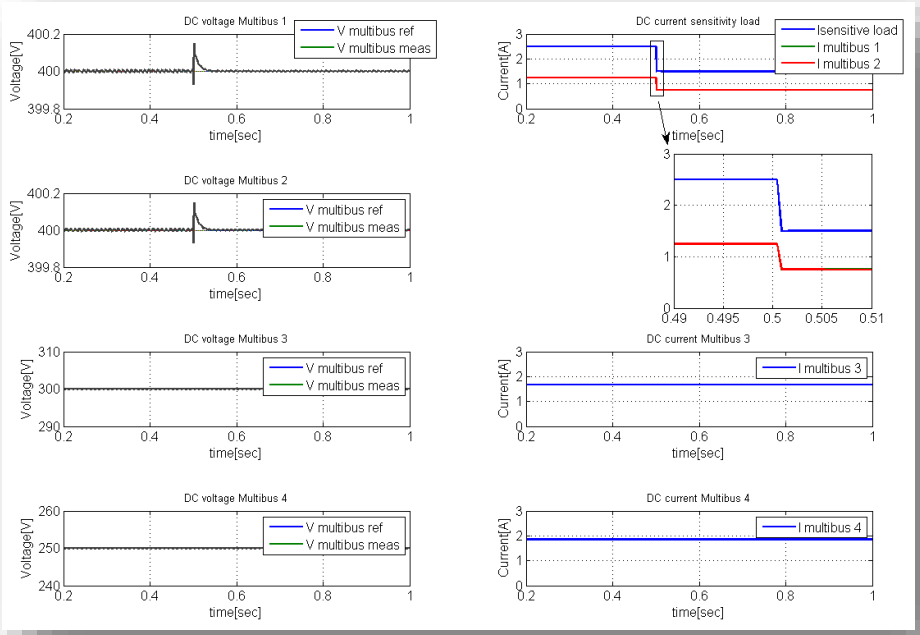

Future Work:
Management of the DC Multibus Fed by the SSBC MMCC Converter and DC Sources together

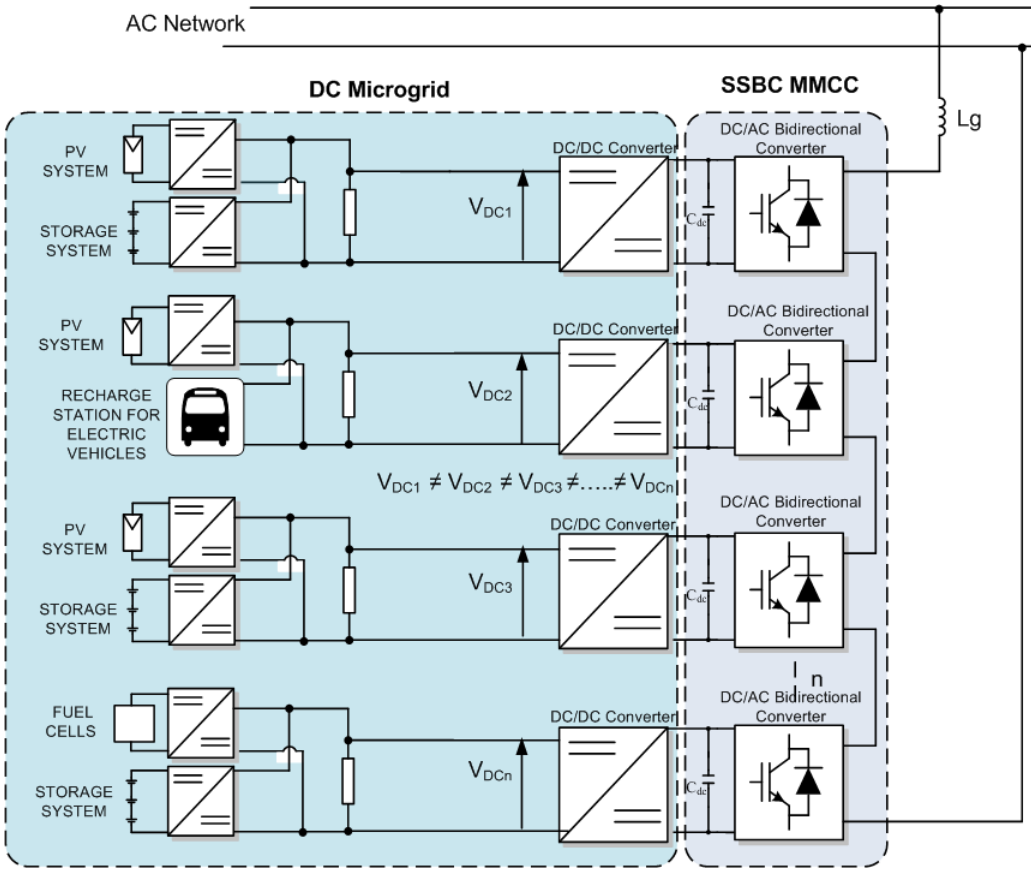

The drawbacks of DC microgrid:

- Circulating currents;
- Instability;
- Oscillations.

DC DROOP CONTROL

Some References:

• M. Liserre, R. A. Mastromauro, A. Nagliero, "Universal operation of small/medium size renewable energy systems", Chapter 9 in "Power Electronics for Renewable Energy Systems, Transportation, and Industrial Applications", First Edition Edited by Haitham Abu-Rub, Mariusz Malinowski and Kamal Al-Haddad © 2014 John Wiley & Sons, Ltd. Published 2014 by John Wiley & Sons, Ltd, pp. 231-269.

•R. A. Mastromauro, M. Liserre, A. Dell'Aquila, "Control Issues in Single-Stage Photovoltaic Systems: MPPT and Current and Voltage Control", IEEE Transactions on Industrial Informatics, vol.8, no.2, pp.241-254, May 2012.

•J. C. Vasquez, R. A. Mastromauro, J. M. Guerrero, M. Liserre, Voltage Support Provided by a Droop-Controlled Multifunctional Inverter, IEEE Transactions on Industrial Electronics, vol.56, no.11, pp.4510-4519, Nov. 2009.

•R. A. Mastromauro, M. Liserre, T. Kerekes, A. Dell'Aquila, "A Single-Phase Voltage Controlled Grid Connected Photovoltaic System with Power Quality Conditioner Functionality", IEEE Transactions on Industrial Electronics, vol.56, no.11, pp.4436-4444, Nov. 2009.

•R. A. Mastromauro, M. Liserre, A. Dell'Aquila, "Study of the Effects of Inductor Nonlinear Behavior on the Performance of Current Controllers for Single-Phase PV Grid Converters", IEEE Transactions on Industrial Electronics, vol. 55, no 5, pp. 2043 – 2052, May.

•A. Nagliero, R. A. Mastromauro, M. Liserre, A. Dell'Aquila, "Monitoring and Synchronization Techniques for Single-Phase PV Systems", Proceedings SPEEDAM 2010, Pisa, Italy, June 2010.

•A. Nagliero, R. A. Mastromauro, V.G. Monopoli, M. Liserre, A. Dell'Aquila, "Analysis of a universal inverter working in grid-connected, stand-alone and micro-grid", Proceedings ISIE 2010, Bari, Italy, July 2010.

•M. Rizo, E. Bueno, A. Dell'Aquila, M. Liserre, R. A. Mastromauro "Generalized Controller for Small Wind Turbines Working Grid-Connected and Stand-Alone", Proceedings ICCEP 2011, Ischia, Italy, June 2011, ISBN: 978-142448928-2.

•R. A Mastromauro, N. A Orlando, D. R., Ricchiuto, M. Liserre, A. Dell'Aquila, "Hierarchical Control of a Small Wind Turbine System for Active Integration in LV Distribution Network", Proceedings ICCEP 2013, Alghero, Italy, June 2013.

•D. Ricchiuto, R. A. Mastromauro, M. Liserre, I. Trintis, S. Munk-Nielsen, "Overview of Multi-DC-Bus Solutions for DC Microgrids", Proceedings PEDG 2013, Rogers, Arkansas, USA, July 2013.

•F. A. Gervasio, R. A. Mastromauro, D. Ricchiuto, M. Liserre, "Dynamic Analysis of Active Damping Methods for LCL-filter-based grid converters", Proceedings IECON 2013, Vienna, Austria, November 2013.

•R.A. Mastromauro, "Voltage control of a grid-forming converter for an AC microgrid: a real case study", Proceedings of IET RPG 2014, Naples, September 2014.